Multiple-Description Coding by Dithered Delta-Sigma Quantization

Østergaard, Jan; Zamir, Ram

Multiple-Description Coding by Dithered Delta-Sigma Quantization

Jan Østergaard and Ram Zamir

Abstract

We address the connection between the multiple-description (MD) problem and Delta-Sigma quantization. The inherent redundancy due to oversampling in Delta-Sigma quantization, and the simple linear-additive noise model resulting from dithered lattice quantization, allow us to construct a symmetric MD coding scheme. We show that the use of a noise shaping filter makes it possible to trade off central distortion for side distortion. Asymptotically as the dimension of the lattice vector quantizer and order of the noise shaping filter approach infinity, the entropy rate of the dithered Delta-Sigma quantization scheme approaches the symmetric two-channel MD rate-distortion function for a memoryless Gaussian source and MSE fidelity criterion, at any side-to-central distortion ratio and any resolution. In the optimal scheme, the infinite-order noise shaping filter must be minimum phase and have a piece-wise flat power spectrum with a single jump discontinuity. We further show that the optimal noise-shaping filter of any order can be found by solving a set of Yule-Walker equations, and we present an exact rate-distortion analysis for any filter order, lattice vector quantizer dimension and bit rate. An important advantage of the proposed design is that it is symmetric in rate by construction, and there is therefore no need for source splitting.

Index Terms

delta-sigma modulation, dithered lattice quantization, entropy coding, joint source-channel coding, multiple-description coding, vector quantization.

I. Introduction and Motivation

Delta-Sigma analogue to digital (A/D) conversion is a technique where the input signal is highly oversampled before being quantized by a low resolution quantizer. The quantization noise is then processed by a noise shaping filter which reduces the energy of the so-called in-band noise spectrum, i.e. the part of the noise spectrum which overlaps the spectrum of the input signal. The end result is high bit-accuracy (A/D) conversion even in the presence of imperfections in the analogue components of the system, cf. [1].

The process of oversampling and use of feedback to reduce quantization noise is not limited to A/D conversion of continuous-time signals but is in fact equally applicable to, for example, discrete time signals in which case we will use the term Delta-Sigma quantization. Hence, given a discrete time signal we can apply Delta-Sigma quantization in order to discretize the amplitude of the signal and thereby obtain a digital signal. It should be clear that the process of oversampling is not required in order to obtain a digital signal. However, oversampling leads to a controlled amount of redundancy in the digital signal. This redundancy can be exploited in order to achieve a certain degree of robustness towards a partial loss of information of the signal due to quantization and/or transmission of the digital signal over error-prone channels.

In the information theory community the problem of quantization is usually referred to as a source coding problem whereas the problem of reliable transmission is referred to as a channel coding problem. Their combination then forms a joint source-channel coding problem. The multiple-description (MD) problem [2], which has recently received a lot of attention, is basically a joint source-channel coding problem. The MD problem is concerned with lossy encoding of information for transmission over an unreliable K-channel communication system. The channels may break down resulting in erasures and a loss of information at the receiving side. Which of the $2^K - 1$ non-trivial subsets of the K channels that is working is assumed known at the receiving side but not at the encoder. The problem is then to design an MD system which, for given channel rates, minimizes the distortions due to reconstruction of the source using information from any subsets of the channels. Currently, the achievable MD rate-distortion region is only completely known for the case of two channels, squared-error fidelity criterion and a memoryless Gaussian source [2], [3]. The bounds of [3] have been extended to stationary and smooth sources in [4], [5], where they were proven to be asymptotically tight at high resolution. Inner and outer

bounds to the rate-distortion region for the case of $K > 2$ channels were presented in [6]–[8] but it is not known whether any of the bounds are tight for $K > 2$ channels.

Practical symmetric MD lattice vector quantization (MD-LVQ) based schemes for two descriptions have been introduced in [9], [10], which in the limit of infinite-dimensional lattices and under high-resolution assumptions, approach the symmetric MD rate-distortion bound. An extension to $K \geq 2$ descriptions was presented in [11]–[13]. Asymmetric MD-LVQ allows for unequal side distortions as well as unequal side rates and was first considered in [14], [15] for the case of two descriptions and extended in [13], [16] to the case of $K \geq 2$ descriptions. Common for all of the designs [9]–[12], [14]–[16] is that a central quantizer is first applied on the source after which an index-assignment algorithm maps the reconstruction points of the central quantizer to reconstruction points of the side quantizers, which is an idea that was first presented in [17].

To avoid the difficulty of designing efficient index-assignment algorithms, it was suggested in [18] that the index assignments of a two-description system can be replaced by successive quantization and linear estimation. More specifically, the two side descriptions can be linearly combined and further enhanced by a refinement layer to yield the central reconstruction. The design of [18] suffers from a rate loss of 0.5 bit/dim. at high resolution and is therefore not able to achieve the MD rate-distortion bound. Recently, however, this gap was closed by Chen et al. [19], [20] who recognized that the rate region of the MD problem forms a polymatroid, and showed that the corner points of this rate region can be achieved by successive estimation and quantization. The design of Chen et al. is inherently *asymmetric* in the description rate since any corner point of a non-trivial rate region will lead to asymmetric rates. To symmetrize the coding rates, it is necessary to break the quantization process into additional stages, which is a method known as "source splitting" (following Urbanke and Rimoldi's rate splitting approach for the multiple access channel). When finite-dimensional quantizers are employed, there is a space-filling loss due to the fact that the quantizer's Voronoi cells are finite dimensional and not completely spherical, [21], and as such each description suffers a rate loss. The rate loss of the design given in [19], [20] is that of $2K - 1$ quantizers because source splitting is performed by using an additional $K - 1$ quantizers besides the conventional K side quantizers. In comparison, the designs based on index assignments suffer from a rate loss of only that of K quantizers (actually, for $K = 2$ the space-filling loss is that of two quantizers having spherical Voronoi

cells [9], [10]). An interesting open question is: can we avoid both the complexity of the index assignments and the loss due to source splitting in symmetric MD coding?

Inspired by the works presented in [18]–[20], [22], we present a two-channel MD scheme based on two times oversampled dithered Delta-Sigma quantization, which is inherently symmetric in the description rate and as such there is no need for source splitting. The rate loss when employing finite-dimensional quantizers (in parallel) is therefore given by that of two quantizers. Asymptotically as the dimension of the vector quantizer and order of the noise shaping filter approach infinity, we show that the symmetric two-channel MD rate-distortion function for a memoryless Gaussian source and MSE fidelity criterion can be achieved at any resolution. It is worth emphasizing that our design is not limited to two descriptions but, in fact, an arbitrary number of descriptions can be created simply by increasing the oversampling ratio. However, in this paper, we only prove optimality for the case of two descriptions.

In the Delta-Sigma quantization literature there seems to be a consensus of avoiding long feedback filters. We suspect this is mainly due to the fact that the quantization error in traditional Delta-Sigma quantization is a deterministic non-linear function of the input signal, which makes it difficult to perform an exact system analysis. Thus, there might be concerns regarding the stability of the system. In our work we use dithered (lattice) quantization, so that the quantization error is a stochastic process, independent of the input signal, and the whole system becomes linear. This linearization is highly desirable, since it allows an exact system analysis for any filter order and at any resolution. For finite filter order, we show that the optimal filter coefficients are found by solving a set of Yule-Walker equations. The case of infinite filter order has a very simple solution in the frequency domain, which (for large lattice dimension) guarantees that the proposed scheme achieves the symmetric two-channel MD rate-distortion function [2], [3].

To gain some insight into why this solution is asymptotically optimal, observe that the Delta-Sigma quantization structure resembles the nature of the optimum test channel that achieves the two-channel MD rate-distortion region [2], [3]. This channel (as shown in Fig. 1) has two additive noise branches $U_0 = X + N_0$ and $U_1 = X + N_1$, where the pair (N_0, N_1) is *negatively* correlated. At high resolution conditions and symmetric rates and distortions, the side reconstructions $\hat{X}_0$ and $\hat{X}_1$ become $\hat{X}_0 = U_0$ and $\hat{X}_1 = U_1$, while the central reconstruction $\hat{X}_c$ becomes a simple average, i.e. $\hat{X}_c = (\hat{X}_0 + \hat{X}_1)/2$. We may view the negatively correlated additive noises as adjacent samples of "highpass noise", and the averaging operation of the central reconstruction

as "lowpass filtering". Intuitively, for a fixed side distortion the central distortion is reduced by shaping the spectrum of the noise to be away from the source band (the source component in U_0 and U_1 is the same which amounts to a lowpass signal). Thus, Delta-Sigma quantization provides a time-invariant filter version of this double branch test channel. This is further addressed in Section IV-E.
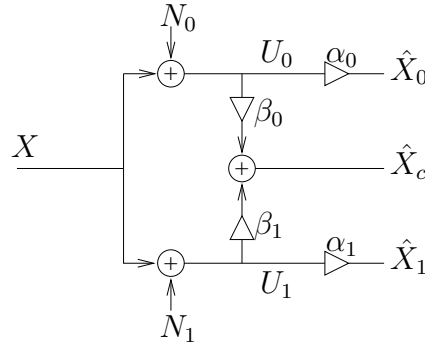

Fig. 1. The MD optimum test channel of Ozarow [3]. At high resolution $\alpha_i = 1$ and $\beta_i = 1/2, i = 0, 1$ so that $\hat{X}_0 = U_0, \hat{X}_1 = U_1$ and $\hat{X}_c = \frac{1}{2}(\hat{X}_0 + \hat{X}_1)$.

Besides the quantizer-based MD schemes mentioned above there exist several other approaches, e.g. MD schemes based on quantized overcomplete expansions [23]–[28]. The works of [23]–[26] are based on finite frame expansions and that of [27], [28] are based on redundant M-channel filter banks.

It is well known that there is a connection between quantized overcomplete expansions and Delta-Sigma quantization, cf. [29]–[31]. Furthermore, as mentioned above, the connection between overcomplete expansions and the MD problem has also been established. Yet, to the best of the authors knowledge, none of the schemes presented in [23]–[28] are able to achieve the above mentioned MD rate-distortion bounds. Furthermore, the use of Delta-Sigma quantization explicitly for MD coding appears to be a new idea. With this paper we show that traditional Delta-Sigma quantization can be recast in the context of MD coding and furthermore, that it provides an optimal solution to the MD problem in the symmetric case.

The paper is structured as follows. In Section II we introduce dithered Delta-Sigma quantization. Section III connects Delta-Sigma quantization with MD coding and presents the main theorem of this work. The proof of the theorem is deferred to Section VI. Section IV presents

an asymptotic description and performance analysis of the proposed scheme in the limit of high dimensional vector quantization and high order noise shaping filter. It is divided into several subsections: Section IV-A gives an intuitive frequency interpretation of MD coding based on Delta-Sigma quantization. In Section IV-B we show that the widely used MD figure of merit, the optimum central-side distortion product, can be achieved at high-resolution conditions with infinite dimension/order Delta-Sigma quantization. In Section IV-C we extend this observation, and prove that with the addition of suitable post-multipliers, the complete symmetric Gaussian rate-distortion function is achievable. Then in Section IV-D we emphasize an important difference between conventional ECDQ for single description and ECDQ for multiple descriptions. We end this section by relating the proposed design to Ozarow's double-branch test channel. The non-asymptotic analysis is presented in Section V. We first present the central and side distortion for an arbitrary noise shaping filter order in Section V-A. Then, in Section V-B, we assess the inherent rate loss due to the use of finite-dimensional vector quantizers, and compare that to the rate loss in other MD coding techniques. We end Section V by deriving the optimal finite-order noise shaping filters. Section VI bridges between Section IV and Section V, and wrap up the proof of the main theorem with a supporting lemma given in the Appendix. An extension to K descriptions is presented in Section VII, and Section VIII shows that the proposed scheme is, in fact, asymptotically optimal at high resolution for any i.i.d. source with finite differential entropy. Finally, Section IX contains the conclusion.

II. DITHERED DELTA-SIGMA QUANTIZATION

Throughout this paper we will use upper case letters for stochastic variables and lower case letters for their realizations. Infinite sequences and L-dimensional vectors will be typed in bold face. We let $X \sim N(0, \sigma_X^2)$ denote a zero-mean Gaussian variable of variance σ_X^2, and $\boldsymbol{X} = \{X_1, X_2, \dots\}$ denote an infinite sequence of independent copies of X. Thus $\boldsymbol{X}$ is an i.i.d. (white) Gaussian process. Moreover, $\boldsymbol{x} = \{x_1, x_2, \dots, \}$ denotes a realization of $\boldsymbol{X}$ where x_k is the kth symbol of $\boldsymbol{x}$.

A. Preliminaries: Entropy-Coded Dithered Quantization

Before introducing our dithered Delta-Sigma quantization system, let us recall the properties of entropy-coded dithered (lattice) quantization (ECDQ) [32]. ECDQ relies upon subtractive
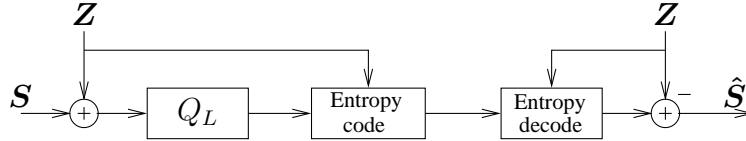
Fig. 2. Entropy-constrained dithered (lattice) quantization (ECDQ). The dither signal $\boldsymbol{Z}$ is assumed known at the decoder. The quantizer Q_L is an L-dimensional lattice vector quantizer and the rate of the entropy coder is given by the entropy of the quantized output of Q_L conditioned upon $\boldsymbol{Z}$.

dither; see Fig. 2. For an L-dimensional input vector $\boldsymbol{S}$, the ECDQ output is given by $\hat{\boldsymbol{S}} = Q_L(\boldsymbol{S} + \boldsymbol{Z}) - \boldsymbol{Z}$, where Q_L denotes an L-dimensional lattice quantizer with Voronoi cells [33]. The dither vector $\boldsymbol{Z}$, which is known to both the encoder and the decoder, is independent of the input signal and previous realizations of the dither, and is uniformly distributed over the basic Voronoi cell of the lattice quantizer. It follows that the quantization error

$$\boldsymbol{E} = \hat{\boldsymbol{S}} - \boldsymbol{S} = Q_L(\boldsymbol{S} + \boldsymbol{Z}) - \boldsymbol{S} - \boldsymbol{Z} \tag{1}$$

is statistically independent of the input signal. Furthermore, $\boldsymbol{E}$ is an i.i.d.-vector process, where each L-block is uniformly distributed over the mirror image of the basic cell of the lattice, i.e., as $-\boldsymbol{Z}$. In particular, it follows that $\boldsymbol{E}$ is a zero-mean white vector with variance σ_E^2 [32], [34].

The average code length of the quantized variables is given by the conditional entropy $H(Q_L(\boldsymbol{S} + \boldsymbol{Z})|\boldsymbol{Z})$ of the quantizer Q_L, where the conditioning is with respect to the dither vector $\boldsymbol{Z}$. It is known that this conditional entropy is equal to the mutual information over the additive noise channel $\boldsymbol{Y} = \boldsymbol{S} + \boldsymbol{E}$ where $\boldsymbol{E}$ (the channel's noise) is distributed as $-\boldsymbol{Z}$; see [32] for details. The coding rate (per L-block) of the quantizer is therefore given by

$$\begin{aligned} H(Q_L(\boldsymbol{S} + \boldsymbol{Z})|\boldsymbol{Z}) &= I(\boldsymbol{S}; \boldsymbol{Y}) \\ &= h(\boldsymbol{S} + \boldsymbol{E}) - h(\boldsymbol{E}) \end{aligned} \tag{2}$$

where $I(\cdot, \cdot)$ denotes the mutual information and $h(\cdot)$ denotes the differential entropy. If subsequent quantizer outputs are entropy-coded jointly, then we must change the blockwise mutual information in the rate formula (2) to the joint mutual information between input-output sequences (if there is no feedback) [32], or to the directed mutual information (if there is feedback) [35], [36]. We shall discuss this issue in more detail in the next section.

If the source $\boldsymbol{S}$ is white Gaussian, then the coding rate (2), normalized per-sample, is upper bounded by

$$\frac{1}{L}H(Q_L(\boldsymbol{S}+\boldsymbol{Z})|\boldsymbol{Z}) \quad \leq \quad \frac{1}{2}\log_2\left(1+\frac{\text{Var}(S_k)}{\sigma_E^2}\right)+\frac{1}{2}\log_2(2\pi eG_L) \qquad (3)$$

$$= \quad R_S(D)+\frac{1}{2}\log_2(2\pi eG_L) \qquad (4)$$

where G_L is the dimensionless normalized second moment of the L-dimensional lattice quantizer Q_L [33]. In the second equality D is the total distortion after a suitable post-filter (multiplier) and $R_S(D)$ is the rate-distortion function of the white Gaussian source S; see [37]. The quantity $2\pi eG_L$ is the space-filling loss of the quantizer and $\frac{1}{2}\log_2(2\pi eG_L)$ is the divergence of the quantization noise from Gaussianity. It follows that it is desirable to have Gaussian distributed quantization noise in order to make G_L as small as possible and thereby drive the rate of the filtered quantizer towards $R_S(D)$. Fortunately, it is known that there exists lattices where $G_L \to 1/2\pi e$ as $L \to \infty$ and the quantization noise of such quantizers is white, and becomes asymptotically (in dimension) Gaussian distributed in the divergence sense [34].

B. Delta-Sigma ECDQ
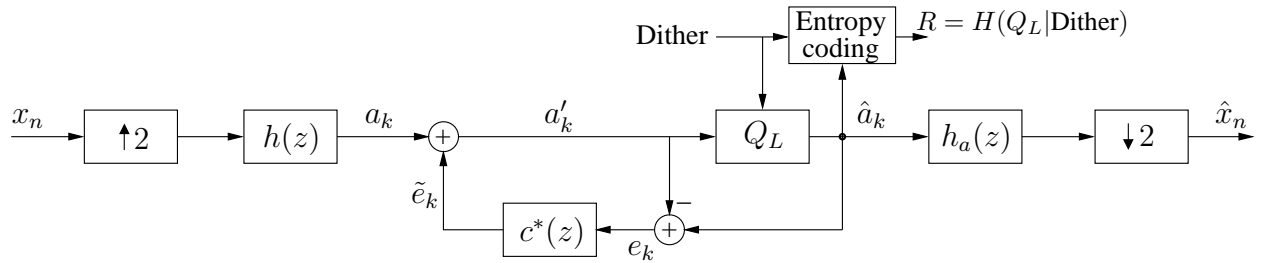
Fig. 3.   Dithered Delta-Sigma quantization.

We are now ready to introduce our dithered Delta-Sigma quantization system, which is sketched in Fig. 3.[1] The input sequence $\boldsymbol{x}$ is first oversampled by a factor of two to produce the oversampled sequence $\boldsymbol{a}$. It follows that $\boldsymbol{a}$ is a redundant representation of the input sequence

---

[1]The Delta-Sigma quantization system shown in Fig. 3 is a discrete-time version of the *general noise-shaping coder* presented in [38]. The system has an equivalent form where the feedback is first subtracted and this difference is then filtered [38].

x, which can be obtained simply by inserting a zero between every sample of x and applying an interpolating (ideal lowpass) filter $h(z)$. For a wide-sense stationary input process X, the resulting oversampled signal A would be wide-sense stationary, with the same variance as the input, and the same power-spectrum only squeezed to half the frequency band as shown in Fig. 4. In particular, a white Gaussian input becomes a half-band low-pass Gaussian process with

$$\text{Var}(A_k) = \text{Var}(X) = \sigma_X^2. \tag{5}$$

At the other end of the system we apply an anti-aliasing filter $h_a(z)$, i.e. an ideal half-band

(a) Spectrum of X (b) Oversampling by two   (c) Spectrum of A
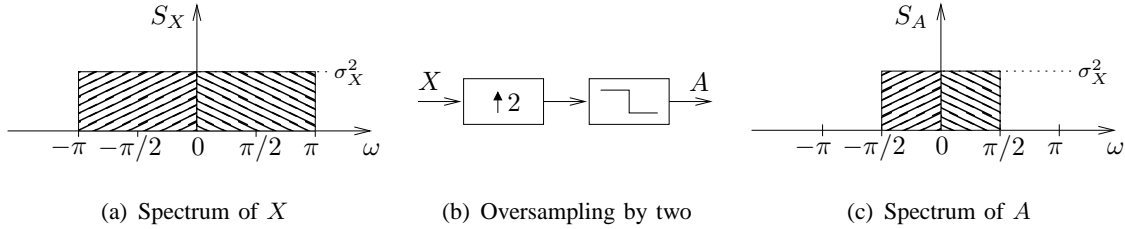
Fig. 4. The power spectrum of (a) the input signal and (c) the oversampled signal. (b) illustrates the oversampling process where the input signal is first upsampled by two and then filtered by an ideal half-band lowpass filter.

lowpass filter, and downsample by two in order to get back to the original sampling rate.

We would like to emphasize that the dithered Delta-Sigma quantization scheme is not limited to oversampling ratios of two. In fact, arbitrary (even fractional) oversampling ratios may be used. This option is discussed further in Section VII.

The oversampled source sequence a is combined with noise feedback $\tilde{e}$, and the resulting signal a' is sequentially quantized on a sample by sample basis using a dithered quantizer. For the simplicity of the exposition we shall momentarily assume scalar quantization, i.e., $L = 1$. The extension to $L > 1$ is discussed in Section II-C. The quantization error e_k of the kth sample, given for a general ECDQ by (1), is fed back through the (causal) filter $c^*(z) = \sum_{i=1}^{p} c_i z^{-i}$ and combined with the next source sample a_{k+1} to produce the next ECDQ input a'_{k+1}. Thus, the output of the quantizer can be written as

$$\hat{a}_k = a'_k + e_k = a_k + \tilde{e}_k + e_k \overset{\Delta}{=} a_k + \epsilon_k \tag{6}$$

where $\tilde{e}(z) = c^*(z)e(z)$ or equivalently

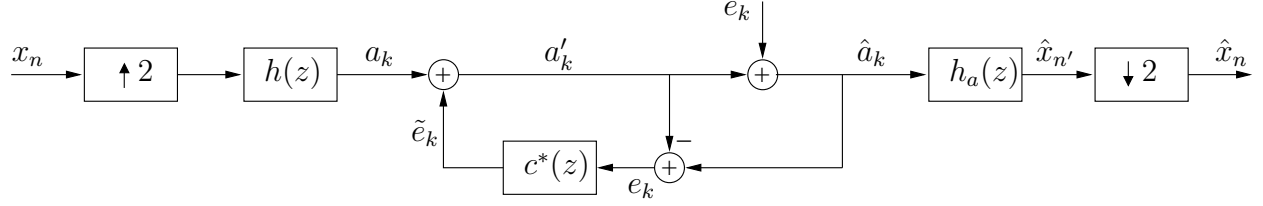$$\tilde{e}_k = \sum_{i=1}^{p} c_i e_{k-i}.$$

Fig. 5.   The dithered quantizer is replaced by the additive noise model.

As explained above, the additive noise model is exact for ECDQ and we can therefore represent the quantization operation as an additive noise channel, as shown in Fig. 5. In view of this linear model, the equivalent reconstruction error in the oversampled domain, denoted ϵ_k in (6), is statistically independent of the source. Thus we call ϵ_k the "equivalent noise". Note that ϵ_k is obtained by passing the quantization error e_k through the equivalent pth order noise shaping filter $c(z)$,

$$c(z) \triangleq \sum_{i=0}^{p} c_i z^{-i} \tag{7}$$

where $c_0 = 1$ so that $c(z) = 1 + c^*(z)$. To see this, notice that the output is $\hat{a}(z) = a(z) + e(z) + c^*(z)e(z)$, and the reconstruction error is therefore given by $\epsilon(z) = c(z)e(z)$, cf. Fig. 6. Since the quantization error e of the ECDQ (1) is white with variance σ_E^2, it follows that the equivalent noise spectrum is given by

$$S_\epsilon(w) = |c(e^{jw})|^2 \sigma_E^2. \tag{8}$$

The fact that the output $\hat{a}_k$ is obtained by passing the quantization error e_k through the noise shaping filter $c(z)$ and adding the result to the input a_k can be illustrated using an equivalent additive noise channel as shown in Fig. 7.
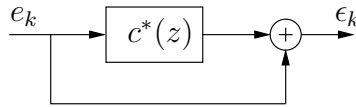

Fig. 6.   The reconstruction error $\epsilon_k = \tilde{e}_k + e_k$ is also called the "equivalent noise", since it can be obtained by passing the quantization error e_k through the "equivalent" noise shaping filter $c(z) = 1 + c^*(z)$.
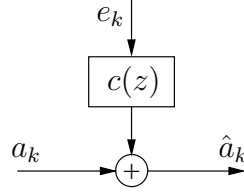
Fig. 7. The equivalent additive noise channel: The output $\hat{a}_k$ is obtained by passing the quantization error e_k through the noise shaping filter $c(z)$ and adding the result to the input a_k.

We may view the feedback filter $c^*(z)$ as if its purpose is to predict the "in-band" noise component of $\tilde{e}_k$ based on the past p quantization error samples $e_{k-1}, e_{k-2}, \ldots, e_{k-p}$. The end result is that the equivalent noise spectrum (8) is shaped away from the in-band part of the spectrum, i.e., from the frequency range $(-\pi/2, +\pi/2)$, as shown in Fig. 8. Note that due to the anti-aliasing filter $h_a(z)$, only the in-band noise determines the overall system distortion. The exact guidelines for this noise shaping are different in the single- and the multiple description cases, and will become clear in the sequel.
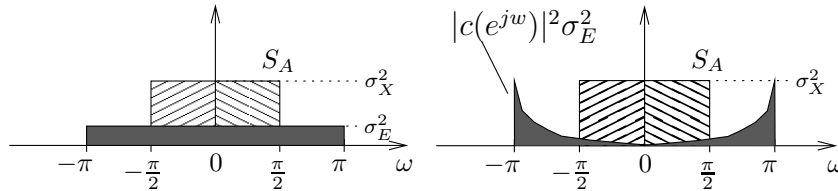
Fig. 8. On the left is illustrated the case where there is no feedback and the quantization noise is therefore flat (in fact white) throughout the entire frequency range. On the right an example of noise shaping is illustrated. The grey-shaded areas illustrate the power spectra of the noise and the hatched areas illustrate the power spectra of the source.

As previously mentioned, if we encode the quantizer output symbols independently, then the rate R of the ECDQ is given by the mutual information between the input and the output of the quantizer.[2] Thus, the rate (per sample) is given by

$$R = I(A_k'; \hat{A}_k) = I(A_k'; A_k' + E_k) \tag{9}$$

[2]We discuss the issue of joint versus memoryless ECDQ in more detail in Section IV-D.

where E_k is independent of the present and past samples of A'_k by the dithered quantization assumption. If A_k and E_k were Gaussian, then we could get

$$R = \frac{1}{2} \log_2 \left(1 + \frac{\text{Var}(A'_k)}{\sigma_E^2} \right) \tag{10}$$

where $\text{Var}(A'_k)$ denotes the variance of the random variable A'_k. At high resolution conditions the variance of the error signal e (and therefore of ϵ) is small compared to the source, so by (5) we have $\text{Var}(A'_k) + \sigma_E^2 \approx \sigma_X^2$ which implies that (10) becomes

$$R \approx \frac{1}{2} \log_2 \left(\frac{\sigma_X^2}{\sigma_E^2} \right) \tag{11}$$

where $\approx$ in (11) is in the sense that the difference goes to zero as $\sigma_E^2 \to 0$.

C. Vector Delta-Sigma Quantization

It should be clear from the discussion about ECDQ in Section II-A that we would like to use high-dimensional quantizers, so that the quantization noise in (9) is indeed approximately Gaussian. However, at first sight, it might appear as the sequential scalar nature of Delta-Sigma quantization prevents the use of anything but scalar quantizers. That this is not so will soon become clear. First, let us consider the scalar case, i.e. $L = 1$. The input to the quantizer is $a'_k = a_k + \sum_{i=1}^p c_i e_{k-i}$ and the output is $\hat{a}_k = a_k + \sum_{i=0}^p c_i e_{k-i}$. Since a'_k is a scalar, the input to the quantizer is a scalar and the quantizer depicted in Fig. 3 is therefore a scalar quantizer. To justify the use of high-dimensional vector quantizers we will consider a setup involving L independent sources.[3] These sources can, for example, be obtained by demultiplexing the scalar process X into L independent parallel i.i.d. processes $X^{(l)} = \{X_{nL+l}\}, \forall n \in \mathbb{Z}$ and $l = 1, \ldots, L$.[4] In this case the nth sample of the lth process $X^{(l)}$ is identical to the $(n \times L + l)$th sample of the original process X. In the case where $L = 2$ we have two independent scalar processes, where $X^{(1)}$ consists of the even samples of X and $X^{(2)}$ consists of the odd samples of X. Let us give an example where $L = 3$ so that we have three processes $X^{(1)}, X^{(2)}$, and $X^{(3)}$. The three processes are each upsampled by a factor of two so that we obtain the three processes $A^{(1)}, A^{(2)}$, and $A^{(3)}$, where each is input to a Delta-Sigma quantization system as shown in Fig. 9. Hence, in this case, three coders are operating in parallel and instead of a single sample a'_k we have a triplet of

---

[3]The idea of applying lattice ECDQ to feedback coding systems in parallel was first presented in [36].

[4]Notice that the delay between two consecutive samples of the lth process will be that of L input samples.

independent samples $(a_k'^{(1)}, a_k'^{(2)}, a_k'^{(3)})$. This makes it possible to apply three-dimensional ECDQ on the vector formed by cascading the triplet of scalars. If L coders are operating in parallel, we can form the set of L independent samples $(a_k'^{(1)}, a_k'^{(2)}, \ldots, a_k'^{(L)})$ and make use of L-dimensional ECDQ on the vector $(a_k'^{(1)}, a_k'^{(2)}, \ldots, a_k'^{(L)})$. In general, we will allow L to become large so that, according to (4) and the paragraph that follows just below (4), the rate loss $\frac{1}{2}\log_2(2\pi e G_L)$ due to the quantization noise being non-Gaussian can be made arbitrarily small. Thus, for large L, E_k in (9) can indeed be approximated as Gaussian noise.

(a) Demultiplexing the i.i.d. source into $L = 3$ independent streams

(b) Applying a three-dimensional lattice quantizer Q_3
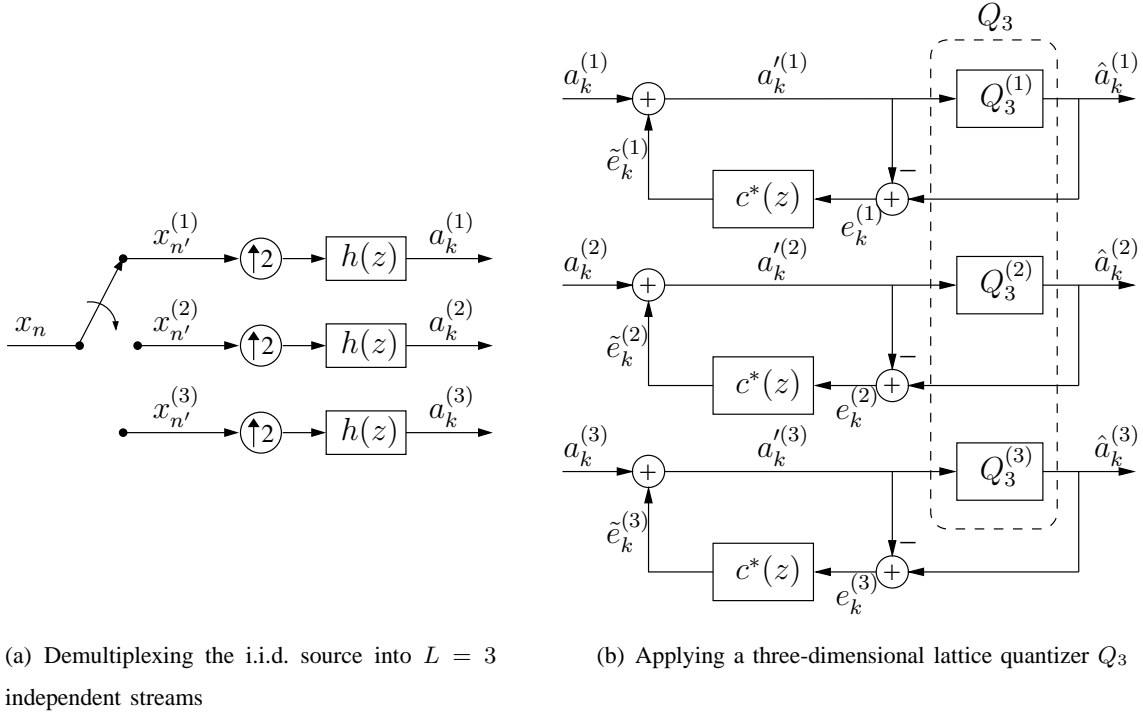
Fig. 9.   The dashed box illustrates that the triplet of scalars $(a_k'^{(1)}, a_k'^{(2)}, a_k'^{(3)})$ are jointly quantized using three-dimensional ECDQ. Notice that we may see the three-dimensional lattice quantizer Q_3 as a composition of three functions where $\hat{a}_k^{(1)} = Q_3^{(1)}(a_k'^{(1)}, a_k'^{(2)}, a_k'^{(3)})$, $\hat{a}_k^{(2)} = Q_3^{(2)}(a_k'^{(1)}, a_k'^{(2)}, a_k'^{(3)})$ and $\hat{a}_k^{(3)} = Q_3^{(3)}(a_k'^{(1)}, a_k'^{(2)}, a_k'^{(3)})$.

III. MULTIPLE-DESCRIPTION CODING

A. MD Delta-Sigma Quantization

In this section we show that the sequential dithered Delta-Sigma quantization system, which is shown in Fig. 3, can be regarded as an MD coding system. For example, in the case of an

oversampling ratio of two, each input sample leads to two output samples and we have in fact a two-channel MD coding system as shown in Fig. 10. As explained in the previous section, we assume that the source is demultiplexed into L parallel streams and that an L-dimensional lattice quantizer is applied on the set of coefficients $(a_k'^{(1)}, \ldots, a_k'^{(L)})$. However, for illustrational and notational convenience, we have only shown a single stream in Fig. 10. It should also be clear that, as L becomes large, the quantization error $E_k = \hat{A}_k - A_k'$ becomes approximately Gaussian distributed in the sense of the mutual information-rate formula (9).

In the MD scheme of Fig. 10, the first description is given by the even outputs of the lattice quantizer and the second description by the odd outputs. Each description is then entropy-coded separately, conditioned upon its own dither, and transmitted to the decoder. Note that although the oversampled signal $\boldsymbol{A}$ has memory, each description is memoryless because of the even/odd splitting of the samples, which corresponds to downsampling by two. It follows that the quantized samples can in fact be entropy coded sample-by-sample, i.e. in a block-wise memoryless fashion, so by (2) the ECDQ rate is given by the block-wise mutual information, normalized per-sample,

$$R = \frac{1}{L} I(\boldsymbol{A}'; \boldsymbol{A}' + \boldsymbol{E}). \tag{12}$$

We further discuss the issue of joint versus memoryless (or independent) ECDQ in Section IV-D.

At the decoder, if both descriptions are received, an anti-aliasing filter $h_a(z)$ (i.e. an ideal half-band lowpass filter) is applied and the signal is then downsampled by two and scaled by β as shown in Fig. 11. If only the even samples are received, we simply scale the signal by α. On the other hand, if only the odd samples are received, we first apply an all-pass filter $h_p(z)$ to correct the phase of the second description and then scale by α. The all-pass filter $h_p(z)$ is needed because the upsampling operation performed at the encoder, i.e. upsampling by two followed by ideal lowpass filtering (sinc-interpolation), shifts the phase of the odd samples. The post multipliers α and β are described in Section IV-C.

The distortion due to reconstructing using both descriptions is traditionally called the central distortion d_c and the distortion due to reconstructing using only a single description is called the side distortion d_s.

B. The MD Rate-Distortion Region

The two-channel MD rate-distortion region is completely characterized only in the quadratic Gaussian case, i.e. the case of memoryless Gaussian sources and MSE fidelity criterion [2], [3].
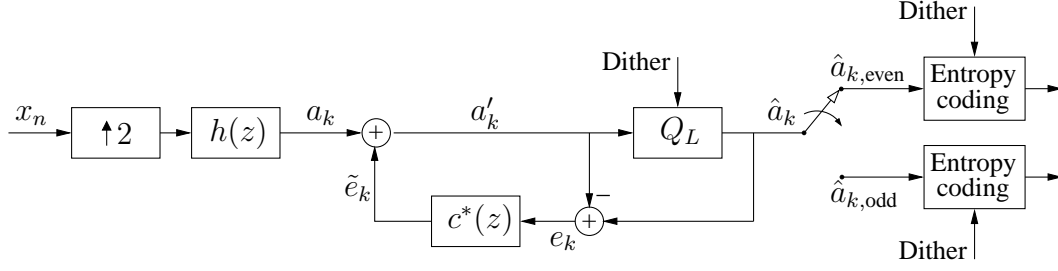
Fig. 10. Two-channel MD coding based on dithered Delta-Sigma quantization: Encoder.
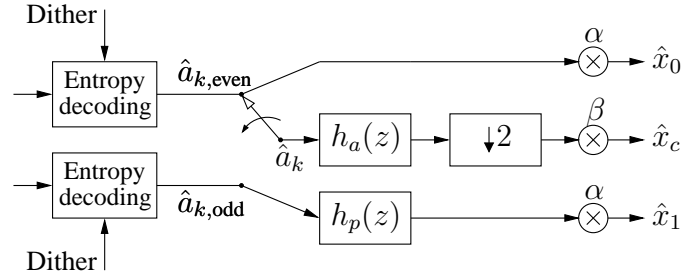
Fig. 11. Two-channel MD coding based on dithered Delta-Sigma quantization: Decoder.

Let us recall the solution to the quadratic Gaussian MD problem, as proven by Ozarow [3], in the *symmetric* case, i.e., when both descriptions have the same rate R and the side distortions are equal. The set of achievable distortions for description rate R is the union of all distortion pairs (d_c, d_s) satisfying

$$d_s \geq \sigma_X^2 2^{-2R} \tag{13}$$

and

$$d_c \geq \frac{\sigma_X^2 2^{-4R}}{1 - (\sqrt{\Pi} - \sqrt{\Delta})^2} \tag{14}$$

where $\Pi = (1 - d_s/\sigma_X^2)^2$ and $\Delta = d_s^2/\sigma_X^4 - 2^{-4R}$.

Based on the results of [3], it was shown in [39] that at high resolution, for fixed central-to-side distortion ratio d_c/d_s, the product of the central and side distortions of an optimal two-channel MD scheme approaches

$$d_c d_s \cong \frac{\sigma_X^4}{4} \frac{1}{1 - d_c/d_s} 2^{-4R} \tag{15}$$

where the approximation $\stackrel{\sim}{=}$ here is in the sense that the ratio between both sides goes to 1 as $d_s \to 0$ (or $R \to \infty$). If $d_s/d_c \gg 1$, i.e., at high side-to-central distortion ratio, this simplifies to

$$d_c d_s \stackrel{\sim}{=} \frac{\sigma_X^4}{4} 2^{-4R}. \tag{16}$$

C. Main Theorem

We now present the main theorem of this work, which basically states that the MD Delta-Sigma quantization scheme (presented in Section III-A) can asymptotically achieve the lower bound of Ozarow's MD distortion region (presented in Section III-B).

Theorem 1: Asymptotically as the filter order p and the vector-quantizer dimension L are going to infinity, the entropy rate and the distortion levels of the dithered Delta-Sigma quantization scheme (of Figs. 10 and 11) achieve the symmetric two-channel MD rate-distortion function (13) – (14) for a memoryless Gaussian source and MSE fidelity criterion, at any side-to-central distortion ratio d_s/d_c and any resolution. Furthermore, the optimal infinite-order noise shaping filter is unique, minimum phase, and its magnitude spectrum $|c(e^{j\omega})|$ is piece-wise flat with a single jump discontinuity at $\omega = \pi/2$.

Before presenting the proof of the theorem, we provide in the following sections a series of supporting lemmas. The proof of the theorem can be found in Section VI.

IV. ASYMPTOTIC DESCRIPTION AND PERFORMANCE ANALYSIS

In this section we concentrate on the asymptotic case where $p, L \to \infty$, i.e. infinite noise shaping filter order and infinite vector quantizer dimension. For analysis purposes, this allows us to assume Gaussian quantization noise in the system model of Fig. 5, with arbitrarily shaped equivalent noise spectrum (8). After gaining some insight from the asymptotic case, we shall turn to treat the case of finite p and L in the next section.

A. Frequency Interpretation of Delta-Sigma Quantization

We first give an intuitive frequency interpretation of the proposed Delta-Sigma quantization scheme. This frequency interpretation reveals that the role of the noise shaping filter is not simply to shape away the quantization noise from the in-band spectrum, as is the case in traditional Delta-Sigma quantization, but rather to delicately control the tradeoff between the in-band noise versus

the out-of-band noise, which translates into a tradeoff between the central and side distortions.[5] This tradeoff is done while keeping the coding rate fixed, which, at least at high resolution, is equivalent to keeping the quantizer variance σ_E^2 fixed. See (11).

Recall that we, at the central decoder, apply an anti-aliasing filter (ideal lowpass filtering) before downsampling. Hence, the central distortion is given by the energy of the quantization noise that falls within the in-band spectrum. The inclusion of a noise shaping filter at the encoder makes it possible to shape away the quantization noise from the in-band spectrum and thereby reduce the central distortion. By increasing the order of the noise shaping filter it is possible to reduce the central distortion accordingly.

It is also interesting to understand what influences the side distortion. Recall that the side descriptions are constructed by using either all odd samples or all even samples of the output A. Hence, we effectively downsample A by a factor of two. It is important to see that this downsampling process takes place without first applying an anti-aliasing filter. Thus, aliasing is inevitable. It follows, that not only the noise which falls within the in-band spectrum contributes to the side distortion but also the noise that falls outside the in-band spectrum (i.e. the out-of-band noise) affects the distortion. Since, in traditional Delta-Sigma quantization, the noise is shaped away from the in-band spectrum as efficiently as possible, the out-of-band noise is likely to be the dominating contributor to the side distortion. We have illustrated this in Fig. 12.

(a) Spectrum of E (b) Spectrum of shaped E
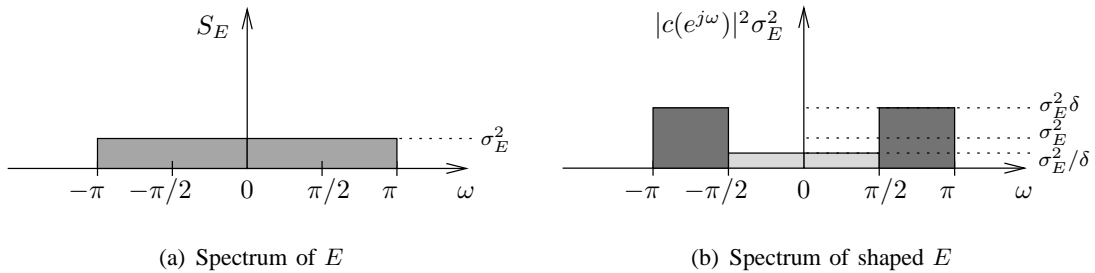
Fig. 12. The power spectrum of (a) the quantization noise (b) the shaped quantization noise. In (b) the energy of the lowpass noise spectrum (the bright region) corresponds to the central distortion and the energy of the full spectrum corresponds to the side distortion.

It should now be clear that, in two-channel MD Delta-Sigma quantization, the role of the

[5]In Section IV-D we show another difference between the noise shaping in traditional Delta-Sigma quantization and MD Delta-Sigma quantization regarding the coding rates.

noise shaping filter is to trade off the in-band noise versus the out-of-band noise. In particular, in the asymptotic case where the order of the noise shaping filter goes to infinity, it is possible to construct a brick-wall filter which has a squared magnitude spectrum of $1/\delta$ in the passband (i.e. for $|\omega| \leq \pi/2$) and of δ in the stopband (i.e. for $\pi/2 < |\omega| < \pi$). In this case, the central distortion is proportional to $1/\delta$ whereas the side distortion is proportional to $1/\delta + \delta$. This situation, which is illustrated in Fig. 12(b), will be discussed in more detail in the next section.

B. Achieving the MD Distortion Product at High Resolution

It is possible to take advantage of the frequency interpretation given in Section IV-A in order to show that the optimum central-side distortion product at high-resolution (15) can be achieved by Delta-Sigma quantization. We later extend this result and show that with suitable post-multipliers at the decoders, optimum performance are achieved at *any* resolution.

Lemma 1: At high resolution and asymptotically as $p, L \to \infty$, the distortion product given by (15) is achievable by Delta-Sigma quantization.

Proof: The central distortion is equal to the total energy P_{d_c} of the in-band noise spectrum where

$$P_{d_c} = \frac{\sigma_E^2}{2\pi} \int_{-\pi/2}^{\pi/2} |c(e^{j\omega})|^2 d\omega. \tag{17}$$

The side distortion is equal to the energy P_{d_s} of the in-band noise spectrum of the side descriptions which contains aliasing due to the subsampling process. Since we downsample by two we have

$$P_{d_s} = \frac{\sigma_E^2}{4\pi} \int_{-\pi}^{\pi} |c(e^{j\omega/2})|^2 + |c(e^{j(\omega/2+\pi)})|^2 d\omega. \tag{18}$$

Let us shape the noise spectrum as illustrated in Fig. 12(b). Thus, we let $|c(e^{j\omega})|^2 = 1/\delta$ for $|\omega| \leq \pi/2$ and $|c(e^{j\omega})|^2 = \delta$ for $\pi/2 < |\omega| < \pi$ where $0 < \delta \in \mathbb{R}$. It follows from (18) that, for any $\delta > 0$, $d_s = \frac{1}{2}\sigma_E^2(\delta + \delta^{-1})$ and from (17) we see that $d_c = \frac{1}{2}\sigma_E^2/\delta$ which yields the distortion product $d_c d_s = \frac{\delta + \delta^{-1}}{4\delta}\sigma_E^4$. From (11) we know that at high resolution $R \approx \log_2(\sigma_X^2/\sigma_E^2)$ (where $\approx$ is in the sense that the difference goes to zero as $R \to \infty$), so that $\sigma_E^4 \cong \sigma_X^4 2^{-4R}$ (where $\cong$ is in the sense that the ratio goes to one as $R \to \infty$). Finally, since $d_c/d_s = \delta^{-1}/(\delta + \delta^{-1})$ it follows that

$$\frac{1}{1 - d_c/d_s} = \frac{\delta + \delta^{-1}}{\delta}$$

which proves the lemma. ∎

C. Optimum Performance for General Resolution

In this section we extend the optimality result of Section IV-B above, and show that the two-channel Delta-Sigma quantization scheme achieves the symmetric quadratic Gaussian rate-distortion function at any resolution.

Let U_i denote the reconstructions before the side post multipliers so that $\hat{X}_i = \alpha U_i, i = 0, 1$, and let $\mathbb{E}$ denote the expectation operator. It can then be shown that $\mathbb{E}XU_i = \sigma_X^2$ and $\mathbb{E}U_i^2 = \sigma_X^2 + \sigma_E^2(\delta + \delta^{-1})/2$. Moreover, let U denote the reconstruction before the central multiplier β. Then $\mathbb{E}U^2 = \sigma_X^2 + \sigma_E^2\delta^{-1}/2$. Finally, let the post multipliers be given by[6]

$$\alpha = \frac{\sigma_X^2}{\sigma_X^2 + \sigma_E^2(\delta + \delta^{-1})/2}$$

and

$$\beta = \frac{\sigma_X^2}{\sigma_X^2 + \sigma_E^2\delta^{-1}/2}.$$

It follows that the side distortion is given by

$$
\begin{aligned}
d_s &= \mathbb{E}(\hat{X}_i - X)^2 \\
&= \mathbb{E}(\alpha U_i - X)^2 \\
&= \sigma_X^2 - 2\alpha\sigma_X^2 + \alpha^2(\sigma_X^2 + \sigma_E^2(\delta + \delta^{-1})/2) \\
&= \frac{\sigma_X^2\sigma_E^2(\delta + \delta^{-1})}{2\sigma_X^2 + \sigma_E^2(\delta + \delta^{-1})}.
\end{aligned}
\tag{19}
$$

Similarly, let $\hat{X}_c = \beta U$ so that the central distortion is given by

$$
\begin{aligned}
d_c &= \mathbb{E}(\hat{X}_c - X)^2 \\
&= \mathbb{E}(\beta U - X)^2 \\
&= \sigma_X^2 + \beta^2(\sigma_X^2 + \sigma_E^2\delta^{-1}/2) - 2\beta\sigma_X^2 \\
&= \frac{\sigma_X^2\sigma_E^2\delta^{-1}}{2\sigma_X^2 + \sigma_E^2\delta^{-1}}.
\end{aligned}
\tag{20}
$$

Lemma 2: For a given description rate R and asymptotically as $p, L \to \infty$ (i.e., assuming Gaussian quantization noise and equivalent noise spectrum as in Fig. 12(b)), the side distortion given by (19) and the central distortion given by (20) achieve the lower bound (14) of Ozarow's symmetric MD distortion region.

---

[6]See Remark 1 in Section V-A for details.

Proof: Recall from Section II, that the rate of memoryless-ECDQ (assuming that the entropy coding is conditioned upon the dither signal and that the dither signal is known at the decoder) is equal to the mutual information between the input and the output of an additive noise channel (12). For large L, this mutual information can be calculated as if the additive noise E_k was approximately Gaussian distributed. It thus follows from (9) and (10) that as $L \to \infty$ the description rate becomes

$$
\begin{aligned}
R &= I(A'_k; \hat{A}_k) \\
&= h(\hat{A}_k) - h(E_k) \\
&= \frac{1}{2}\log_2(2\pi e(\sigma_X^2 + \sigma_E^2(\delta + \delta^{-1})/2)) - \frac{1}{2}\log_2(2\pi e\sigma_E^2) \\
&= \frac{1}{2}\log_2\left(\frac{\sigma_X^2 + \sigma_E^2(\delta + \delta^{-1})/2}{\sigma_E^2}\right).
\end{aligned}
\tag{21}
$$

We can rewrite (21) as

$$
2^{-4R} = \frac{4\delta^2\sigma_E^4}{(2\sigma_X^2\delta + \sigma_E^2\delta^2 + \sigma_E^2)^2}.
\tag{22}
$$

By use of (19) and (22) we then get

$$
\Delta = \frac{\sigma_E^4(\delta^4 - 2\delta^2 + 1)}{(2\sigma_X^2\delta + \sigma_E^2\delta^2 + \sigma_E^2)^2}
$$

and

$$
\Pi = \frac{4\delta^2\sigma_X^4}{(2\sigma_X^2\delta + \sigma_E^2\delta^2 + \sigma_E^2)^2}
$$

so that

$$
1 - (\sqrt{\Pi} - \sqrt{\Delta})^2 = \frac{4\sigma_E^2\delta^2(2\sigma_X^2\delta + \sigma_E^2)}{(2\sigma_X^2\delta + \sigma_E^2\delta^2 + \sigma_E^2)^2}.
\tag{23}
$$

Finally, inserting (23) in (14) leads to

$$
\frac{\sigma_X^2 2^{-4R}}{1 - (\sqrt{\Pi} - \sqrt{\Delta})^2} = \frac{\sigma_X^2\sigma_E^2}{2\sigma_X^2\delta + \sigma_E^2}
$$

which is identical to (20) and therefore proves the lemma.   ■

D. Comparison with a Single-Description System with Joint Entropy Coding

We previously saw that, in the SD case, only the in-band noise spectrum affects the distortion, whereas the complete noise spectrum affects the MD distortions. Specifically, the in-band noise spectrum determines the central distortion and the sum of the in-band and out-of-band noise

spectrum determines the side distortion. We can show a similar relationship with respect to the rates. First, notice from (21) that the description rate in the MD case depends upon the complete noise spectrum.[7] We will now show that in the SD case, if we apply *joint* entropy coding of the quantizer outputs, that is, we let the entropy coder take advantage of the memory inside the oversampled source, then the rate of the Delta-Sigma quantization scheme would be independent of the out-of-band noise spectrum.

Recall that for jointly-coded ECDQ within a feedback loop, the coding rate is given by the *directed* mutual information rate, that is, [36],

$$
\begin{aligned}
\bar{I}(A'_k \to A'_k + E_k) &= I(A'_k; A'_k + E_k | A'_{k-1} + E_{k-1}, A'_{k-2} + E_{k-2}, \dots) \\
&= h(A'_k + E_k | A'_{k-1} + E_{k-1}, A'_{k-2} + E_{k-2}, \dots) - h(E_k) \\
&\stackrel{(a)}{=} h(A_k + \boldsymbol{\epsilon}_k | A_{k-1} + \boldsymbol{\epsilon}_{k-1}, A_{k-2} + \boldsymbol{\epsilon}_{k-2}, \dots) - h(E_k) \qquad (24) \\
&\stackrel{(b)}{=} \bar{h}(A + \boldsymbol{\epsilon}) - \bar{h}(\boldsymbol{\epsilon}) \\
&= \bar{I}(A; A + \boldsymbol{\epsilon})
\end{aligned}
$$

where $\bar{h}(\cdot)$ and $\bar{I}(\cdot)$ denote the entropy rate and mutual information rate, respectively. In the equations above (a) follows since $A'_k = A_k + \tilde{E}_k$ and $\boldsymbol{\epsilon}_k = \tilde{E}_k + E_k$. In (b) we used the fact that E_k is the prediction error of $\boldsymbol{\epsilon}_k$ given its past so that $h(E_k)$ is the entropy rate of $\boldsymbol{\epsilon}$, i.e. $\bar{h}(\boldsymbol{\epsilon}) = \bar{h}(E_k) = h(E_k)$.

Asymptotically as $L \to \infty$, the quantization noise becomes approximately Gaussian distributed, and the equivalent ECDQ channel is AWGN. Recall that, for a Gaussian process, disjoint frequency bands are statistically independent. Therefore, since the input A is lowpass, the mutual-information rate is independent of the out-of-band part of the noise process $\boldsymbol{\epsilon}$. Thus, the coding rate is independent of the out-of-band noise spectrum.

E. Relation to Ozarow's Double Branch Test Channel

Let us now revisit Ozarow's double branch test channel as shown in Fig. 1. In this model the noise pair (N_0, N_1) is negatively correlated (except from the case of no-excess marginal rates, in which case the noises are independent). Notice that this is in line with the above

---

[7]Recall that the side distortion is associated with the entire noise spectrum through the sum $(\delta + \delta^{-1})/2$. This sum is also part of the rate expression in (21).

observations, since the highpass nature of the noise shaping filter causes adjacent noise samples to be negatively correlated. The more negatively correlated they are, the greater is the ratio of side distortion over central distortion. Furthermore, at high resolution, the filters in Ozarow's test channel degenerate and the central reconstruction is simply given by the average of the two side channels. This averaging operation can be seen as a lowpass filtering operation, which leaves the signal (since it is lowpass) and the in-band noise intact but removes the out-of-band noise.

More formally, for the symmetric case (where $\sigma_N^2 = \sigma_{N_i}^2, i = 0, 1$ and ρ is the correlation coefficient of the noises), we have the following high-resolution relationships between (ρ, σ_N^2) of Ozarow's test channel and (δ, σ_E^2) of the proposed Delta-Sigma quantization scheme.

Lemma 3: At high-resolution conditions, we have

$$\sigma_E^2 = \sigma_N^2 \sqrt{1 - \rho^2} \tag{25}$$

and

$$\delta = \frac{\sqrt{1 - \rho}}{\sqrt{1 + \rho}}. \tag{26}$$

Proof: From [4], [5] it follows that Ozarow's sum rate $R_0 + R_1$ satifies

$$R_0 + R_1 \geq I(X; X + N_0) + I(X; X + N_1) + I(X + N_0; X + N_1)$$

$$= I(X; X + N_0) + I(X; X + N_1) + I(N_0; N_1)$$

$$= I(X; X + N_0) + I(X; X + N_1) + \frac{1}{2} \log_2 \left(\frac{1}{1 - \rho^2} \right)$$

which in the symmetric case and at high resolution conditions is approximately given by

$$2R = \log_2(\sigma_X^2 / \sigma_N^2) + \frac{1}{2} \log_2 \left(\frac{1}{1 - \rho^2} \right). \tag{27}$$

Using that $R = \frac{1}{2} \log_2(\sigma_X^2 / \sigma_E^2)$ in (27) leads to

$$\log_2(\sigma_E^2 / \sigma_N^2) = \frac{1}{2} \log_2(1 - \rho^2)$$

and it follows that

$$\sigma_E^2 = \sigma_N^2 \sqrt{1 - \rho^2}$$

which proves (25).

The MMSE when estimating X from two jointly Gaussian noisy observations $U_i = X + N_i, i = 0, 1$ (where the Gaussian noises have equal variance), is given by

$$\text{MMSE} = \frac{\sigma_N^2(1 + \rho)}{\sigma_N^2(1 + \rho) + 2}$$

which, at high-resolution conditions, simplifies to

$$\text{MMSE} \approx \frac{1}{2}\sigma_N^2(1+\rho). \tag{28}$$

Recall that the central distortion of the Delta-Sigma-quantization scheme, at high-resolution conditions, is given by

$$d_c = \frac{1}{2}\sigma_E^2\delta^{-1}. \tag{29}$$

Equating (28) and (29) and inserting (25) lead to

$$\delta = \frac{\sqrt{1-\rho^2}}{1+\rho} = \frac{\sqrt{(1-\rho)(1+\rho)}}{1+\rho} = \frac{\sqrt{1-\rho}}{\sqrt{1+\rho}}$$

which proves (26). ∎

V. Non Asymptotic Analysis

In this section we consider the case of finite lattice vector quantizer dimension and finite noise shaping filter order.

A. Central and Side Distortions

Lemma 4: For any filter order $p \in \mathbb{Z}^+$, the central distortion, at high-resolution conditions, is given by

$$d_c = \frac{\sigma_E^2}{2}\sum_{i=0}^{p}\sum_{j=0}^{p}\text{sinc}\left(\frac{i-j}{2}\right)c_ic_j. \tag{30}$$

Proof: Let $\epsilon_n = \hat{x}_n - x_n$ be the error signal. Without loss of generality, we may view the upsampling operation followed by ideal lowpass filtering as an over-complete expansion of the source, where the infinite-dimensional analysis frame vectors with coefficients $\tilde{h}_{k,n} = \text{sinc}(\frac{n-k}{2})$ are translated sinc functions[8]. Thus, adopting the notation of [31], we have that

$$a_k = \sum_{n=-\infty}^{\infty} x_n\text{sinc}\left(\frac{n-k}{2}\right)$$

---

[8]The sinc function is defined by

$$\text{sinc}(x) \triangleq \begin{cases} \frac{\sin(\pi x)}{\pi x}, & x \neq 0 \\ 1, & x = 0. \end{cases}$$

and the synthesis filters are given by $h_{k,n} = \frac{1}{2}\text{sinc}(\frac{n-k}{2})$, so that

$$x_n = \frac{1}{2} \sum_{k=-\infty}^{\infty} a_k \text{sinc}\left(\frac{n-k}{2}\right).$$

Since $\hat{a}_k = a_k + e_k + \sum_{i=1}^{p} c_i e_{k-i}$, the error $\epsilon_n = \hat{x}_n - x_n$ is given by

$$\epsilon_n = \sum_{k=-\infty}^{\infty} h_{k,n} \left(\sum_{i=0}^{p} c_i e_{k-i} \right). \tag{31}$$

The (per sample) mean squared error (MSE) is (by use of (31)) given by

$$\mathbb{E}\epsilon_n^2 = \mathbb{E}\left[\left(\sum_{k=-\infty}^{\infty} h_{k,n} \left(\sum_{i=0}^{p} c_i E_{k-i} \right) \right)^2 \right]$$

$$= \mathbb{E}\left[\sum_{k=-\infty}^{\infty} \sum_{l=-\infty}^{\infty} h_{k,n} h_{l,n} \left(\sum_{i=0}^{p} c_i E_{k-i} \right) \left(\sum_{i=0}^{p} c_i E_{l-i} \right) \right]$$

$$= \frac{1}{4}\mathbb{E}\left[\sum_{k=-\infty}^{\infty} \sum_{l=-\infty}^{\infty} \text{sinc}\left(\frac{n-k}{2}\right) \text{sinc}\left(\frac{n-l}{2}\right) \left(\sum_{i=0}^{p} c_i E_{k-i} \right) \left(\sum_{i=0}^{p} c_i E_{l-i} \right) \right]$$

$$= \frac{1}{4} \sum_{k=-\infty}^{\infty} \sum_{l=-\infty}^{\infty} \text{sinc}\left(\frac{n-k}{2}\right) \text{sinc}\left(\frac{n-l}{2}\right) \sum_{i=0}^{p} \sum_{j=0}^{p} c_i c_j \mathbb{E}[E_{k-i} E_{l-j}]$$

$$= \frac{1}{4} \sum_{k=-\infty}^{\infty} \text{sinc}\left(\frac{n-k}{2}\right) \sum_{i=0}^{p} \sum_{j=0}^{p} c_i c_j \mathbb{E}\left[E_{k-i} \sum_{l=-\infty}^{\infty} \text{sinc}\left(\frac{n-l}{2}\right) E_{l-j} \right]$$

$$\overset{(a)}{=} \frac{1}{4} \sum_{k=-\infty}^{\infty} \text{sinc}\left(\frac{n-k}{2}\right) \sum_{i=0}^{p} \sum_{j=0}^{p} c_i c_j \mathbb{E}\left[E_{k-i}^2 \text{sinc}\left(\frac{n-k-i+j}{2}\right) \right]$$

$$\overset{(b)}{=} \frac{\sigma_E^2}{2} \sum_{i=0}^{p} \sum_{j=0}^{p} \text{sinc}\left(\frac{i-j}{2}\right) c_i c_j,$$

where (a) follows from the fact that $\mathbb{E}E_{k-i}E_{l-j}$ is non-zero only when $l - j = k - i$ which implies that $l = k - i + j$ and (b) is due to the following property of the sinc function

$$\sum_{k=-\infty}^{\infty} \text{sinc}\left(c_0 - \frac{k}{r}\right) \text{sinc}\left(c_0 - \frac{k-c_1}{r}\right) = r \, \text{sinc}\left(\frac{c_1}{r}\right).$$

■

Lemma 5: For any filter order $p \in \mathbb{Z}^+$, the side distortion, at high-resolution conditions, is given by

$$d_s = \sigma_E^2 \sum_{i=0}^{p} c_i^2. \tag{32}$$

Proof: Follows from Lemma 4 by noticing that since we only receive either all odd samples or all even samples, we should only sum over terms where the lag $|i - j|$ is even. However, all cross-terms, $c_i c_j, i \neq j$, vanish since $\text{sinc}(x/2) = 0$ for $x = \pm 2, \pm 4, \ldots$, so only the $p + 1$ auto-terms, $c_i^2, i = 0, \ldots, p$, contribute to the distortion. In addition, we make use of the following property of the sinc function

$$\sum_{k=-\infty}^{\infty} \text{sinc}\left(\frac{xk}{r}\right) \text{sinc}\left(\frac{xk - c}{r}\right) = \frac{r}{x}\text{sinc}\left(\frac{c}{r}\right). \tag{33}$$

∎

Lemma 6: The optimal multipliers, at general resolution and finite noise shaping filter order p, is given by

$$\alpha = \frac{\sigma_X^2}{\sigma_X^2 + \sigma_E^2 \sum_{j=0}^{p} c_j^2} \tag{34}$$

and

$$\beta = \frac{\sigma_X^2}{2\sigma_X^2 + \sigma_E^2 \sum_{i=0}^{p} \sum_{j=0}^{p} \text{sinc}(\frac{i-j}{2})c_i c_j}. \tag{35}$$

Proof: Let U_i denote the reconstruction before the multiplier α such that $\hat{X}_i = \alpha U_i, i = 0, 1$. It should be clear that $\mathbb{E}XU_i = \sigma_X^2$.[9] Recall from the proof of Lemma 5 that the auto-correlation of the even lags of U_i vanish so that

$$\mathbb{E}U_i^2 = \sigma_X^2 + \sigma_E^2 \sum_{j=0}^{p} c_j^2. \tag{36}$$

Since, $\mathbb{E}[X|U_i] = \alpha U_i$, it follows that

$$\alpha = \frac{\sigma_X^2}{\sigma_X^2 + \sigma_E^2 \sum_{j=0}^{p} c_j^2}.$$

Let U denote the reconstruction before the central post multiplier β. From (30) and its proof, it can be seen that

$$\mathbb{E}U^2 = \sigma_X^2 + \frac{\sigma_E^2}{2} \sum_{i=0}^{p} \sum_{j=0}^{p} \text{sinc}\left(\frac{i - j}{2}\right) c_i c_j. \tag{37}$$

Using that $\mathbb{E}[X|U] = \beta U$, we get

$$\beta = \frac{\sigma_X^2}{\sigma_X^2 + \frac{\sigma_E^2}{2} \sum_{i=0}^{p} \sum_{j=0}^{p} \text{sinc}(\frac{i-j}{2})c_i c_j}.$$

[9]The even samples are noisy versions of X where the noise is independent of X. The odd samples are noisy and phase shifted versions of X. However, the phase shift is corrected by the all-pass filter $h_p(z)$ before the post multiplier. Thus, $\mathbb{E}XU_i = \sigma_X^2, i = 0, 1$.

∎

Remark 1: In Section (IV-C) we claimed that, in the asymptotic case of $p \to \infty$, we have $\mathbb{E}U_i^2 = \sigma_X^2 + \sigma_E^2(\delta + \delta^{-1})/2$ and $\mathbb{E}U^2 = \sigma_X^2 + \sigma_E^2 \delta^{-1}/2$. That this is so, follows trivially from (36) and (37) by noting that $\sum_{i=0}^p c_i^2 = (\delta + \delta^{-1})/2$ and $\sum_{i=0}^p \sum_{j=0}^p c_i c_j = \delta^{-1}$.

B. Rate Loss: Comparison with Other MD Coding Techniques

Existing state-of-the-art MD coding schemes, which under certain asymptotics, achieve the quadratic Gaussian MD rate-distortion region, include the index-assignment based schemes by Servetto, Vaishampayan and Sloane [9], [10] as well as the source-splitting approach of Chen, Tian, Berger, and Hemami [19], [20]. Common for these designs (including the proposed Delta-Sigma quantization based design) is that they all rely on lattice vector quantizers and in the limit as the dimension of the quantizers approach infinity, the information-theoretic bounds can be achieved. In practice, however, the schemes employ finite-dimensional vector quantizers and there is therefore a gap between the practical rate-distortion performance and the information theoretic rate-distortion bounds. In other words, the practical schemes suffer a rate loss. In this section we assess the rate loss of the different schemes.

At high-resolution conditions, it was shown in [9], [10] that the total rate loss (or sum rate loss) of the index-assignment based scheme is twice that of a single-description "quantizer" having spherical Voronoi cells. Thus, the rate loss R_L (at high resolution) is given by

$$R_L = \log_2(G(S_L)2\pi e) \tag{38}$$

where $G(S_L)$ is the dimensionless normalized second moment of an L-dimensional hyper-sphere [33].

On the other hand, the rate loss of the source-splitting approach is that of three single-description lattice vector quantizers because source splitting is performed by using an additional quantizer besides the two conventional side quantizers [19], [20]. Thus, we have

$$R_L = 1.5 \log_2(G(\Lambda_L)2\pi e).$$

Finally, for the proposed scheme, asymptotically as $p \to \infty$, the central and side distortions depend only upon δ and the second-order statistics of the source and the noise, i.e. σ_X^2 and σ_E^2. Thus, the particular distributions of the source and the noise are irrelevant. However, these

distributions affect the rate. Specifically, let us assume the source is Gaussian.[10] Then, at high-resolution conditions, we have equality in (4). Thus, in this case, the rate loss is given by the divergence of the quantization noise from Gaussianity. In other words, the rate loss is identical to that of two L-dimensional lattice vector quantizers. Hence,[11]

$$R_{\mathrm{L}} = \log_2(G(\Lambda_L)2\pi e). \tag{39}$$

We have illustrated these rate losses in Fig. 13 where we assume that the lattice vector quantizers being used are the best known in their dimensions, cf. [33].

Remark 2: It should be noted that the rate loss for the source-splitting approach is exact without additional asymptotic assumptions. However, the rate loss for the index-assignment based schemes is only exact for large side-to-central distortions ratios, i.e. asymptotically as d_s/d_c becomes large. The rate loss for the proposed scheme becomes exact asymptotically as $p \to \infty$. Of course, practical situations require a finite distortion ratio d_s/d_c and a finite-order feedback filter. Thus, an additional rate loss can be expected.

C. Coefficients of the Noise Shaping Filter

In this subsection we derive the optimal filter coefficients for the pth order noise shaping filter. We first present Lemma 7, which consider the case where we minimize the central distortion and do not care about the side distortion. This is optimal for the SD setup. However, in an MD setup one might wish to trade off central distortion for side distortion while keeping the filter order fixed. For example, it is often desired to minimize a weighted sum between the central and side distortions. In this case the cost functional J to be minimized is given by

$$J = \lambda_c d_c + \lambda_s d_s \tag{40}$$

where $0 \leq \lambda_c, \lambda_s \in \mathbb{R}$. The case of $\lambda_c \neq 0$ and $\lambda_s = 0$ corresponds to optimal central distortion leading to the filter coefficients of Lemma 7 whereas the case of $\lambda_c = 0$ and $\lambda_s \neq 0$ corresponds to optimal side distortion. By Lemma 8 we find the filter coefficients, which minimize (40).

---

[10]Note that, at high-resolution conditions, the proposed scheme is universal in the sense that the rate loss is independent of the source distribution as long as $h(X) < \infty$ and X is i.i.d.

[11]It is worth emphasizing, that the power spectrum of each description is flat (in fact white). Thus, the individual components are i.i.d. It follows that, there is no additional rate loss by performing separate entropy coding of the quantized source vectors within a description (compared to joint entropy coding).
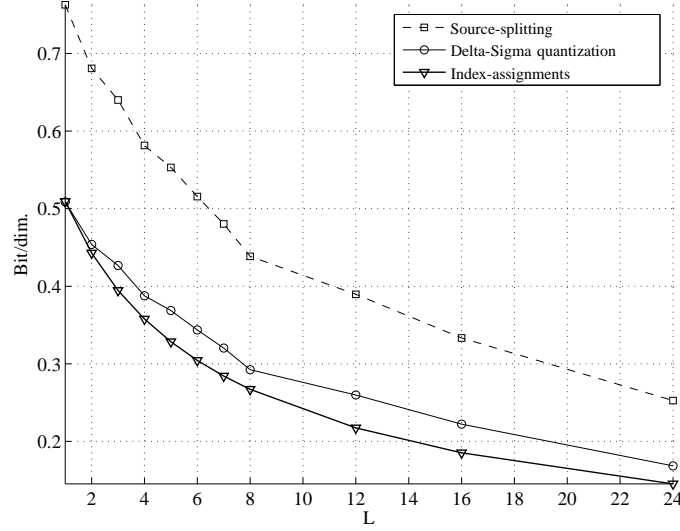
Fig. 13.   Rate loss (in bit/dim.) of the different two-channel MD schemes as a function of the dimension of the best known lattice vector quantizer.

Lemma 7: For any $p \in \mathbb{Z}^+$ the filter coefficients $\boldsymbol{c} = (c_1, \ldots, c_p)$ which minimize the central distortion (30) are

$$\boldsymbol{c} = -\boldsymbol{G}^{-1}\boldsymbol{g}$$

where $\boldsymbol{g}$ is the p-vector with elements $g_i = \mathrm{sinc}(i/2), i = 1, \ldots, p$, and $\boldsymbol{G}$ is the $p \times p$ autocorrelation matrix with elements $G_{i,j} = \mathrm{sinc}((i - j)/2)$, where $i, j \in \{1, \ldots, p\}$.

Proof: From (30) it follows that d_c is given by

$$
\frac{\sigma_E^2}{2}\sum_{i=0}^{p}\sum_{j=0}^{p}\mathrm{sinc}\left(\frac{i-j}{2}\right)c_i c_j = \frac{\sigma_E^2}{2}(1 + 2\sum_{i=1}^{p}\mathrm{sinc}(i/2)c_i + \sum_{i=1}^{p}\sum_{j=1}^{p}\mathrm{sinc}((i-j)/2)c_i c_j)
$$
$$
= \frac{\sigma_E^2}{2}(1 + 2\boldsymbol{c}^T\boldsymbol{g} + \boldsymbol{c}^T\boldsymbol{G}\boldsymbol{c}). \tag{41}
$$

The optimal filter coefficients are found by solving the differential equation

$$\frac{\partial(1 + 2\boldsymbol{c}^T\boldsymbol{g} + \boldsymbol{c}^T\boldsymbol{G}\boldsymbol{c})}{\partial\boldsymbol{c}} = \boldsymbol{0}$$

to which the solutions are easily found to be

$$\boldsymbol{G}\boldsymbol{c} = -\boldsymbol{g}$$

which leads to the desired result whenever the inverse of $\boldsymbol{G}$ exists.   ∎

Remark 3: The filter coefficients given by Lemma 7 are in fact equivalent to those presented in [38] where the in-band noise of a noise shaping coder is minimized in the frequency domain.

Lemma 8: For any $p \in \mathbb{Z}^+$ let $\boldsymbol{g}$ and $\boldsymbol{G}$ be defined as in Lemma 7. Then the filter coefficients $\boldsymbol{c} = (c_1, \ldots, c_p)$ which minimize (40) are given by

$$\boldsymbol{c} = -(\boldsymbol{G} + 2\frac{\lambda_s}{\lambda_c}\boldsymbol{I})^{-1}\boldsymbol{g} \tag{42}$$

where $\boldsymbol{I}$ is the $p \times p$ identity matrix.

Proof: First, let us rewrite the side distortion (32) as $d_s = \sigma_E^2 \sum_{i=0}^{p} c_i^2 = \sigma_E^2(1 + \boldsymbol{c}^T\boldsymbol{c})$.[12] We then expand (40) as

$$\begin{aligned}
\lambda_c d_c + \lambda_s d_s &= \frac{\sigma_E^2}{2}\left(\lambda_c(1 + 2\boldsymbol{c}^T\boldsymbol{g} + \boldsymbol{c}^T\boldsymbol{G}\boldsymbol{c}) + 2\lambda_s(1 + \boldsymbol{c}^T\boldsymbol{c})\right) \\
&= \frac{\sigma_E^2}{2}\left(\lambda_c + 2\lambda_s + 2\lambda_c\boldsymbol{c}^T\boldsymbol{g} + \boldsymbol{c}^T(\lambda_c\boldsymbol{G} + 2\lambda_s\boldsymbol{I})\boldsymbol{c}\right).
\end{aligned} \tag{43}$$

It is now easy to show that the vector $\boldsymbol{c}$ which minimizes (43) is given by (42) whenever the inverse of $\boldsymbol{G}$ exists. ∎

Remark 4: Adding the diagonal matrix $2\lambda_s/\lambda_c\boldsymbol{I}$ to $\boldsymbol{G}$, as done in Lemma 8, has the advantage that the resulting matrix is non-singular also for large filter orders, e.g. $p \approx 5000$. This is a useful property for practical applications, since $\boldsymbol{G}$ easily becomes ill-conditioned also at low filter orders, e.g. $p \approx 20$.

Example 1: Let $\lambda_c = 100$ and $\lambda_s = 1$ so that $10\log_{10}(\lambda_c/\lambda_s) = 20$ dB. Furthermore, let $p = 100$. For this example, the squared magnitude spectrum of the optimal noise shaping filter $c(z)$ given by Lemma 8 is shown in Fig. 14. Notice that it resembles a step function with about 20 dB difference between the low and high frequency bands.

VI. PROOF OF THEOREM 1

We are now in a position to wrap up the proof of Theorem 1. Lemma 2 actually shows that it is possible to achieve the quadratic Gaussian rate-distortion function if we replace the ECDQ by a Gaussian noise, and the equivalent noise spectrum (8) by a brick wall spectrum. This can be viewed as setting the lattice quantizer dimension L and the feedback filter order p to be *equal to infinity*. Thus, what is still missing is the characterization of the limit behavior of the coding rate as $L \to \infty$, and the distortion as $p \to \infty$.

---

[12]Without loss of generality, we can assume that the post multipliers α and β are included within the weights λ_s and λ_c.
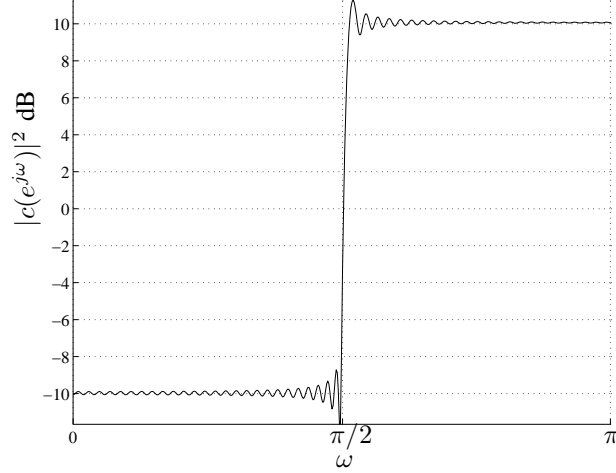
Fig. 14.   The squared magnitude spectrum $|c(e^{j\omega})|^2$ of the optimal noise shaping filter $c(z)$ (obtained by Lemma 8) with filter order $p = 100$ and $\lambda_0/\lambda_1 = 100$.

An upper bound for the rate loss with respect to the vector quantizer dimension L follows from (3). In fact, at high-resolution, we have equality in (4) for any L. Thus, as discussed in Section V-B, the redundancy of the dithered delta-sigma quantization system above the optimum coding rate in Lemma 2 is given by $\log(G(\Lambda_L)2\pi e)$ (see (39)), which goes to zero as $\log(L)/L$ [34].

Regarding the filter order p, let $S_\epsilon(\omega)$ denote the power spectrum of the ideal infinite-order noise shaping filter, which is optimal and unique as proven by Lemma 9 in the Appendix. Thus, $S_\epsilon(\omega)$ is piece-wise flat with a jump discontinuity at $\omega/2$, cf. Fig. 12(b). For such a function, point-wise convergence of the Fourier coefficients cannot be guaranteed. However, we do have convergence in the mean square sense [40]. Specifically, let $S_\epsilon^{(p)}(\omega)$ denote the pth order Fourier approximation to $S_\epsilon(\omega)$. Then [40]

$$\lim_{p\to\infty} \int_{|\omega|\leq\pi} \left| S_\epsilon(\omega) - S_\epsilon^{(p)}(\omega) \right|^2 d\omega = 0 \tag{44}$$

which asserts that the limit for $p \to \infty$ exists. In addition, it can be shown that the error (MSE) of the pth order Fourier approximation of this step function is of the order $\mathcal{O}(1/p)$ [41]. It follows that, since $d_c = \int_{|\omega|\leq\pi/2} S_\epsilon^{(p)}(\omega)d\omega$ and $d_s = \int_{|\omega|\leq\pi/2} S_\epsilon^{(p)}(\omega)d\omega + \int_{\pi/2<|\omega|<\pi} S_\epsilon^{(p)}(\omega)d\omega$, the desired continuity in the limit is assured. In other words, for any $\zeta > 0$, there exists a $1 \leq p < \infty$ such that the pair (d_s, d_c) satisfies Ozarow's optimal solutions given by (13)

and (14) to within a ζ margin, where $\zeta \to 0$ as $p \to \infty$. Specifically, for any $d_s \geq \sigma_X^2 2^{-2R} + \zeta$ we have

$$\frac{\sigma_X^2 2^{-4R}}{1 - (\sqrt{\Pi} - \sqrt{\Delta})^2} \leq d_c \leq \frac{\sigma_X^2 2^{-4R}}{1 - (\sqrt{\Pi} - \sqrt{\Delta})^2} + \zeta. \tag{45}$$

This completes the proof of Theorem 1.

VII. EXTENSION TO $K > 2$ DESCRIPTIONS

In this section we present a straight-forward extension of the proposed design to K descriptions.[13] The basic idea is to change the oversampling ratio from two to K and then decide which output samples should make up a description.[14] When dealing with K descriptions, $2^K - 1$ distinct subsets of descriptions can be created. Thus, the design of the decoders is generally more complex for greater K. For example, if two out three descriptions are received, aliasing is unavoidable (as was the case for $K = 2$ descriptions). Moreover, due to the fractional (non-uniform) downsampling process, the simple brick-wall lowpass filter operation is not necessarily the optimal reconstruction rule. In fact, the optimal reconstruction rule depends not only upon the number of received descriptions but (generally) also upon which descriptions are received. However, in this section we will restrict attention to cases leading to uniform sampling.[15] Thus, the design of the decoders is simplified.

We use the previously presented Delta-Sigma quantization scheme (of Figs. 10 and 11) but oversample now by K instead of two. More specifically, let us assume that $K = 4$ and that every fourth sample make up a description. We note that the extension to an arbitrary number of descriptions is straight forward. We consider only the cases that leads to uniform (non-fractional) downsampling, i.e. reception of any single description, every other description (i.e. two out of four), or all four descriptions.

It can easily be seen that if we receive all four descriptions, the central distortion d_c is given by the noise that falls within the in-band spectrum. In other words,

$$d_c = \frac{1}{2\pi} \int_{-\pi/4}^{\pi/4} S_\epsilon(\omega) d\omega \tag{46}$$

---

[13]For the case of $K > 2$ descriptions, we do not claim optimality.

[14]Note that even fractional oversampling ratios can be used.

[15]We suspect that results from non-uniform sampling or non-uniform filterbank theory will prove advantageous for constructing the optimal decoders in the most general situation. However, this is a topic of future research.

where $S_\epsilon(\omega) = |c(e^{j\omega})|^2 \sigma_E^2$ denotes the power spectrum of the shaped noise. Similarly, when receiveiving two out of four descriptions (i.e. one of the pair of descriptions (0,2) or (1,3)) the side distortion d_2 is given by

$$d_2 = \frac{1}{2\pi} \int_{-\pi/4}^{\pi/4} S_\epsilon(\omega)d\omega + \frac{1}{2\pi} \int_{\frac{3}{4}\pi \leq |\omega| < \pi} S_\epsilon(\omega)d\omega \tag{47}$$

where the latter term is due to aliasing (since we downsample by two without applying any anti-aliasing filter). Finally, if we receive only a single description and thereby downsample by four, the side distortion d_1 is given by the complete shaped noise spectrum, that is

$$d_1 = \frac{1}{2\pi} \int_{-\pi}^{\pi} S_\epsilon(\omega)d\omega. \tag{48}$$

Once again, we let $p \to \infty$ and take advantage of the frequency-domain interpretation, which we previously presented for the case of two descriptions. We divide the power spectrum of the shaped noise into three flat regions as shown in Fig. 15. The low frequency band (i.e. $|\omega| \leq \pi/4$) is of power δ_0, the middle band (i.e. $\pi/4 < |\omega| \leq 3\pi/4$) is of power δ_2, and the high band (i.e. $3\pi/4 < |\omega| < \pi$) is of power δ_1. With this choice of noise shaping, we guarantee that $c(z)$ is minimum phase simply by letting $\delta_2 = 1/\sqrt{\delta_0\delta_1}$ so that $\int_{-\pi}^{\pi} \log_2 S_\epsilon(\omega)d\omega = 0$. From (46) – (48) it follows that[16]

$$d_c = \frac{\sigma_E^2}{4}\delta_0, \tag{49}$$

$$d_2 = \frac{\sigma_E^2}{4}(\delta_0 + \delta_1)$$
$$= d_c + \frac{\sigma_E^2}{4}\delta_1 \tag{50}$$

and

$$d_1 = \frac{\sigma_E^2}{4}(\delta_0 + \delta_1 + 2/\sqrt{\delta_0\delta_1})$$
$$= d_2 + \frac{\sigma_E^2}{2\sqrt{\delta_0\delta_1}}. \tag{51}$$

The description rate follows easily from previous results since the source is memoryless after downsampling. Specifically, it is easy to show that

$$R = \frac{1}{2}\log_2\left(\frac{\sigma_X^2 + \sigma_E^2(\delta_0 + \delta_1 + 2/\sqrt{\delta_0\delta_1})/4}{\sigma_E^2}\right)$$
$$\approx \frac{1}{2}\log_2(\sigma_X^2/\sigma_E^2),$$

[16]For clarity we have excluded the post multipliers, which are required for optimal reconstruction at general resolution. At high resolution conditions, the post multipliers become trivial and will not affect the distortions.
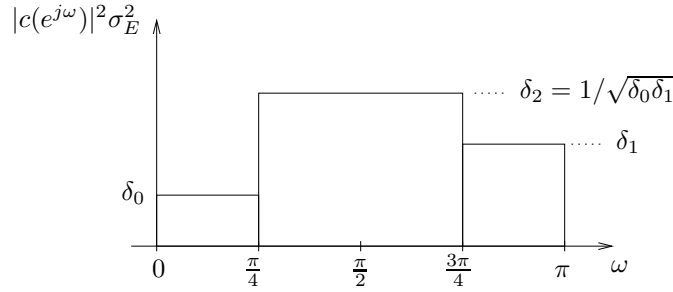
Fig. 15.   An example of a shaped noise power spectrum $|c(e^{j\omega})|^2\sigma_E^2$ for $K = 4$ descriptions.

where the approximation becomes exact at high resolution.

It is worth emphasizing that in this example we have two controlling parameters, i.e. δ_0 and δ_1, where $\delta_0 \leq 1$ and $\delta_0\delta_1 \leq 1$. It is therefore possible to achieve almost arbitrary distortion ratios $d_1/d_2, d_1/d_c$ and d_2/d_c. This gives an advantage over existing designs. For example, the source-splitting design of Chen et al. [19], [20] is based on a single controlling parameter ρ in the symmetric case. The parameter ρ describes here the correlation between the noises of the K descriptions just as was the case with Ozarow's solution for the two-channel problem. In order to increase the number of controlling parameters, it appears to be necessary to exploit the concept of binning as was done in the distributed MD approach of Pradhan et al. [7], [8]. The index-assignment based schemes for $K \geq 2$ descriptions by Østergaard et al. [11]–[13] also rely upon a single controlling parameter N (in the symmetric case). Here N describes the sublattice index of a nested sublattice. It is also possible to obtain additional controlling parameters for the index-assignment based schemes by using the binning approach of [7], [8], cf. [13], [42].

For the case of distributed source coding problems, e.g. the Wyner-Ziv problem, efficient binning schemes based on nested lattice codes have been proposed by Zamir et al. [43], [44]. However, these binning schemes are not (directly) applicable for the MD problem.[17] An alternative binning approach based on generalized coset codes has recently been proposed by Pradhan and Ramchandran [45]. It was indicated in [45] that the coset-based binning approach is applicable also for MD coding but the inherent rate loss was not addressed. Thus, the problem of designing efficient capacity achieving binning codes for the MD problem appears to be unsolved.

---

[17]By making use of time-sharing, it is possible to apply the binning schemes presented in [43], [44] to the MD problem.

From a practical point of view, it is therefore desirable to avoid binning. While the proposed MD design based on Delta-Sigma quantization avoids binning, we do not know whether there is a price to be paid in terms of rate loss. We leave it as a topic of future research, to construct optimal reconstruction rules for the cases of non-uniform downsampling and furthermore addressing the issue whether the achievable K-channel rate-distortion region coincide with the largest known, i.e. those obtained by Pradhan et al. [7], [8].

VIII. Universality of Dithered Delta-Sigma Quantization

We end this paper by a remark about the universality of the proposed scheme at high resolution. First, note that the central and side distortions depend only upon the second-order statistics of the source and the quantization noise, i.e. σ_X^2 and σ_E^2, and as such not on the Gaussianity of the source. Second, independent of the source distribution, the distribution of the quantization noise becomes approximately Gaussian distributed (in the divergence sense) in the limit of high vector quantizer dimension L. Finally, the ECDQ is allowed to encode each description according to its entropy. Thus, the coding rate is equal to the mutual information (12) of the source over the Gaussian test channel. For memoryless sources of equal variances, this coding rate is upper bounded by that of the Gaussian source. Moreover, Zamir proved in [4] that Ozarow's test channel becomes asymptotically optimal in the limit of high resolution for any i.i.d. source provided it has a finite differential entropy. Thus, since the dithered Delta-Sigma quantization scheme resembles Ozarow's test channel in the limit as $p, L \to \infty$, we deduce that the proposed scheme becomes asymptotically optimal for general i.i.d. sources with finite differential entropy.

A delicate point to note, though, is that due to the sinc interpolation, the odd samples might not be i.i.d. and joint entropy coding within the packet is necessary in order to be optimal. Specifically, with joint entropy coding the rate is given by the directed mutual information formula (24) applied to the sub-sampled source $\hat{A}_{k,odd}$. The resulting rate for the odd packet is $\bar{h}(A_{k,odd}) - h(E_k)$, which at high resolution conditions is $\approx h(X) - \frac{1}{2}\log_2(2\pi e \sigma_E^2)$, as desired [4].

In fact, if we have a source with memory, and we allow joint entropy coding within each of the two packets, then a similar derivation shows that we would achieve rate $R \approx \bar{h}(X) - \frac{1}{2}\log_2(2\pi e \sigma_E^2)$ in each packet. This rate is the mutual information rate of the source over the Gaussian test channel. Since Ozarow's test channel is asymptotically optimal in the limit of high

resolution for any stationary source with finite differential entropy rate, [5], it follows that the proposed scheme is optimal for such sources as well.

IX. CONCLUSION

We proposed a symmetric two-channel MD coding scheme based on dithered Delta-Sigma quantization. We showed that for large vector quantizer dimension and large noise shaping filter order it was possible to achieve the symmetric two-channel MD rate-distortion function for a memoryless Gaussian source and MSE fidelity criterion. The construction was shown to be inherently symmetric in the description rate and there was therefore no need for source-splitting as were the case with existing related designs. It was shown that by simply increasing the oversampling ratio from two to K it was possible to construct K descriptions. Moreover, the distortions resulting when reconstructing using distinct subsets of the K descriptions could, in certain cases, be separately controlled via the noise shaping filter without the use of binning. The design of optimal reconstruction rules for $K > 2$ descriptions was left as an open problem.

APPENDIX

The noise shaping filter $c(z)$ found by Lemma 8 results from solving a set of Yule-Walker equations. It is known that this filter is unique and furthermore, that it is minimum-phase [46]. Moreover, the noise shaping filter used in the proof of Lemma 2 to show achievability of the quadratic Gaussian rate-distortion function is of infinite order and satisfies

$$\frac{1}{2\pi} \int_{-\pi}^{\pi} \log_2 |c(e^{j\omega})|^2 d\omega = 0. \tag{52}$$

It follows that the area under $\log_2 |c(e^{j\omega})|^2$ is equally distributed above and below the 0 dB line, which is a unique property of minimum-phase filters [47]. In fact, the following Lemma proves that, in order for $c(z)$ to be optimal, it must be of infinite-order and minimum phase.

Lemma 9: In order to achieve the quadratic Gaussian rate-distortion function, it is required that the noise shaping filter $c(z)$ is of infinite order, minimum-phase, and have a piece-wise flat power spectrum of power δ^{-1} in the lowpass band (i.e. for $|\omega| < \pi/2$ or equivalently for $|f| \leq 1/2$) and of power δ in the highpass band (i.e. for $\pi/2 < |\omega| < \pi$ or equivalently $1/4 < |f| < 1/2$) where $1 \leq \delta \in \mathbb{R}$.

Proof: A minimum-phase filter $H(z)$ with power spectrum $S(f) = |H(e^{j2\pi f})|^2, -1/2 < f \leq 1/2$ satisfies

$$e^{\int_{-1/2}^{1/2} \ln S(f)df} = |h_0|^2$$

where h_0 is the zero-tap of the filter. It is also known that the zero-tap of a minimum-phase filter is strictly larger than the zero-tap of a non-minimum-phase filter having the same power spectrum [48]. It follows that, for an arbitrary filter $H(z)$ with power spectrum $S(f)$ and zero-tap h_0

$$e^{\int_{-1/2}^{1/2} \ln S(f)df} \geq |h_0|^2$$

with equality if and only if $H(z)$ is minimum phase. Furthermore, from the geometric-arithmetic means inequality it can be shown that

$$\int_{-1/2}^{1/2} S(f)df \geq 2\sqrt{\int_{|f| \leq 1/4} S(f)df \int_{1/4 < |f| < 1/2} S(f)df} \tag{53}$$

$$\geq e^{\int_{-1/2}^{1/2} \ln S(f)df} \tag{54}$$

$$\geq 1 \tag{55}$$

where we used the fact that, in our case, $h_0 = 1$ and where we have equality all the way if and only if the filter $H(z)$ is minimum phase and the power spectrum consists of two flat regions; $S(f) = k_0$ for $|f| \leq 1/4$ and $S(f) = k_1$ for $1/4 < |f| < 1/2$. Notice that, for the filter to be minimum-phase, we must have $k_0 = 1/k_1$. Let us now fix the side-to-central distortion ratio $d_s/d_c = \gamma$, where $1 \leq \gamma \in \mathbb{R}$. Then, since $d_c = \int_{|f| \leq 1/4} S(f)df$ and $d_s = \int_{|f| \leq 1/4} S(f)df + \int_{1/4 < |f| < 1/2} S(f)df$ it follows that

$$\frac{\int_{1/4 < |f| < 1/2} S(f)df}{\int_{|f| \leq 1/4} S(f)df} = \gamma - 1. \tag{56}$$

Using (56) in the right-hand-side of (53) leads to the following two inequalities

$$d_c \geq \frac{1}{2} \frac{1}{\sqrt{\gamma - 1}} \tag{57}$$

and

$$d_s \geq \frac{1}{2}\sqrt{\gamma - 1} + \frac{1}{2} \frac{1}{\sqrt{\gamma - 1}} \tag{58}$$

where we have equality in both (57) and (58) (at the same time) if and only if the filter is minimum phase and the power spectrum is a two-step function, i.e. it has constant power $k_0 =$

$\delta^{-1} = 1/\sqrt{\gamma - 1}$ through-out the lowpass band and $k_1 = \delta$ through-out the highpass band.[18] Thus, for a fixed distortion ratio γ, any other filter shape must necessarily lead to a greater distortion. To complete the proof, we remark that in order to have such an ideal brick-wall power spectrum, the order of the filter must necessarily be infinite. ∎

ACKNOWLEDGMENT

REFERENCES

[1] J. C. Candy and G. C. Temes, eds., *Oversampling Delta-Sigma Data Converters: Theory, Design and Simulation*. IEEE Press, 1992.

[2] A. A. E. Gamal and T. M. Cover, "Achievable rates for multiple descriptions," *IEEE Trans. Inf. Theory*, vol. IT-28, pp. 851 – 857, November 1982.

[3] L. Ozarow, "On a source-coding problem with two channels and three receivers," *Bell System Technical Journal*, vol. 59, pp. 1909 – 1921, December 1980.

[4] R. Zamir, "Gaussian codes and shannon bounds for multiple descriptions," *IEEE Trans. Inf. Theory*, vol. 45, pp. 2629 – 2636, November 1999.

[5] R. Zamir, "Shannon type bounds for multiple descriptions of a stationary source," *Journal of Combinatorics, Information and System Sciences*, pp. 1 – 15, December 2000.

[6] R. Venkataramani, G. Kramer, and V. K. Goyal, "Multiple description coding with many channels," *IEEE Trans. Inf. Theory*, vol. 49, pp. 2106 – 2114, September 2003.

[7] S. S. Pradhan, R. Puri, and K. Ramchandran, "n-channel symmetric multiple descriptions–part I: (n, k) source-channel erasure codes," *IEEE Trans. Inf. Theory*, vol. 50, pp. 47 – 61, January 2004.

[8] R. Puri, S. S. Pradhan, and K. Ramchandran, "n-channel symmetric multiple descriptions- part II: An achievable rate-distortion region," *IEEE Trans. Inf. Theory*, vol. 51, pp. 1377 – 1392, April 2005.

[9] S. D. Servetto, V. A. Vaishampayan, and N. J. A. Sloane, "Multiple description lattice vector quantization," in *Proc. Data Compression Conf.*, pp. 13 – 22, March 1999.

[10] V. A. Vaishampayan, N. J. A. Sloane, and S. D. Servetto, "Multiple-description vector quantization with lattice codebooks: Design and analysis," *IEEE Trans. Inf. Theory*, vol. 47, pp. 1718 – 1734, July 2001.

[11] J. Østergaard, J. Jensen, and R. Heusdens, "n-channel symmetric multiple-description lattice vector quantization," in *Proc. Data Compression Conf.*, pp. 378 – 387, March 2005.

[12] J. Østergaard, J. Jensen, and R. Heusdens, "n-channel entropy-constrained multiple-description lattice vector quantization," *IEEE Trans. Inf. Theory*, vol. 52, pp. 1956 – 1973, May 2006.

[13] J. Østergaard, *Multiple-description lattice vector quantization*. PhD thesis, Delft University of Technology, Delft, The Netherlands, June 2007. Available online: http://arxiv.org/abs/0707.2482.

---

[18]In fact we only require that $\operatorname{ess\,inf} S(f) = \delta^{-1}$ for $|f| \leq \frac{1}{4}$ and $\operatorname{ess\,sup} S(f) = \delta$ for $\frac{1}{4} < |f| < \frac{1}{2}$.

[14] S. N. Diggavi, N. J. A. Sloane, and V. A. Vaishampayan, "Design of asymmetric multiple description lattice vector quantizers," in *Proc. Data Compression Conf.*, pp. 490 – 499, March 2000.

[15] S. N. Diggavi, N. J. A. Sloane, and V. A. Vaishampayan, "Asymmetric multiple description lattice vector quantizers," *IEEE Trans. Inf. Theory*, vol. 48, pp. 174 – 191, January 2002.

[16] J. Østergaard, R. Heusdens, and J. Jensen, "n-channel asymmetric multiple-description lattice vector quantization," in *Proc. IEEE Int. Symp. Information Theory*, pp. 1793 – 1797, September 2005.

[17] V. A. Vaishampayan, "Design of multiple description scalar quantizers," *IEEE Trans. Inf. Theory*, vol. 39, pp. 821 – 834, May 1993.

[18] Y. Frank-Dayan and R. Zamir, "Dithered lattice-based quantizers for multiple descriptions," *IEEE Trans. Inf. Theory*, vol. 48, pp. 192 – 204, January 2002.

[19] J. Chen, C. Tian, T. Berger, and S. S. Hemami, "A new class of universal multiple description lattice quantizers," in *Proc. IEEE Int. Symp. Information Theory*, (Adelaide, Australia), pp. 1803 – 1807, September 2005.

[20] J. Chen, C. Tian, T. Berger, and S. S. Hemami, "Multiple description quantization via Gram-Schmidt orthogonalization," *IEEE Trans. Inf. Theory*, vol. 52, pp. 5197 – 5217, December 2006.

[21] A. Gersho, "Asymptotically optimal block quantization," *IEEE Trans. Inf. Theory*, vol. IT-25, pp. 373 – 380, July 1979.

[22] N. S. Jayant, "Subsampling of a DPCM speech channel to provide two self-contained, half-rate channels," *Bell Syst. Tech. Jour.*, vol. 60, pp. 501 – 509, April 1981.

[23] V. K. Goyal, J. Kovačević, and M. Vetterli, "Multiple description transform coding: Robustness to erasures using tight frame expansions," in *Proc. IEEE Int. Symp. Information Theory*, p. 408, August 1998.

[24] V. K. Goyal, J. Kovačević, and M. Vetterli, "Quantized frame expansions as source channel codes for erasure channels," in *Proc. Data Compression Conf.*, pp. 326 – 335, March 1999.

[25] P. A. Chou, S. Mehrotra, and A. Wang, "Multiple description decoding of overcomplete expansions using projections onto convex sets," in *Proc. Data Compression Conf.*, pp. 72 – 81, March 1999.

[26] V. Goyal, J. Kovačević, and J. Kelner, "Quantized frame expansions with erasures," *Journal of Appl. and Comput. Harmonic Analysis*, vol. 10, pp. 203–233, May 2001.

[27] P. L. Dragotti, J. Kovačević, and V. K. Goyal, "Quantized oversampled filter banks with erasures," in *Proc. Data Compression Conf.*, pp. 173 – 182, March 2001.

[28] J. Kovačević, P. L. Dragotti, and V. K. Goyal, "Filter bank frame expansions with erasures," *IEEE Trans. Inf. Theory*, vol. 48, pp. 1439 – 1450, June 2002.

[29] H. Bölcskei and F. Hlawatsch, "Noise reduction in oversampled filter banks using predictive quantization," *IEEE Trans. Inf. Theory*, vol. 47, pp. 155 – 172, January 2001.

[30] P. T. Boufounos and A. V. Oppenheim, "Compensation of coefficient erasures in frame representations," in *Proc. IEEE Int. Conf. Acoustics, Speech, and Signal Processing*, vol. 3, pp. 848 – 851, May 2006.

[31] P. T. Boufounos and A. V. Oppenheim, "Quantization noise shaping on arbitrary frame expansions," *EURASIP Journal on Applied Signal Processing*, vol. 2006, pp. 1 – 12, 2006.

[32] R. Zamir and M. Feder, "On universal quantization by randomized uniform/lattice quantizer," *IEEE Trans. Inf. Theory*, vol. 38, pp. 428 – 436, March 1992.

[33] J. H. Conway and N. J. A. Sloane, *Sphere packings, Lattices and Groups*. Springer, 3rd ed., 1999.

[34] R. Zamir and M. Feder, "On lattice quantization noise," *IEEE Trans. Inf. Theory*, vol. 42, pp. 1152 – 1159, July 1996.

[35] J. L. Massey, "Causality, feedback and directed information," in *Proc. Int. Symp. on Info. Th. & its Appls.*, pp. 303 – 305, November 1990.

[36] R. Zamir, Y. Kochman, and U. Erez, "Achieving the Gaussian rate-distortion function by prediction," *IEEE Trans. Inf. Theory*. Submitted.

[37] R. Zamir and M. Feder, "Information rates of pre/post-filtered dithered quantizers," *IEEE Trans. Inf. Theory*, vol. 42, pp. 1340 – 1353, September 1996.

[38] S. K. Tewksbury and R. W. Hallock, "Oversampled, linear predictive and noise-shaping coders of order $N > 1$," in *Oversampling Delta-Sigma Data Converters: Theory, Design and Simulation* (J. C. Candy and G. C. Temes, eds.), pp. 139 – 149, IEEE Press, 1992.

[39] V. A. Vaishampayan, J.-C. Batllo, and A. Calderbank, "On reducing granular distortion in multiple description quantization," in *Proc. IEEE Int. Symp. Information Theory*, p. 98, August 1998.

[40] G. Bachman, L. Narici, and E. Beckenstein, *Fourier and wavelet analysis*. Springer, 2000.

[41] M. Vetterli, "Wavelets, approximation, and compression," *IEEE Signal Processing Magazine*, vol. 18, pp. 59 – 73, September 2001.

[42] J. Østergaard, R. Heusdens, and J. Jensen, "Source-channel erasure codes with lattice codebooks for multiple description coding," in *Proc. IEEE Int. Symp. Information Theory*, pp. 2324 – 2328, July 2006.

[43] R. Zamir and S. Shamai, "Nested linear/lattice codes for Wyner-Ziv encoding," in *Proc. IEEE Information theory workshop*, pp. 92 – 93, June 1998.

[44] R. Zamir, S. Shamai, and U. Erez, "Nested linear/lattice codes for structured multiterminal binning," *IEEE Trans. Inf. Theory*, vol. 48, pp. 1250 – 1276, June 2002.

[45] S. S. Pradhan and K. Ramchandran, "Generalized coset codes for distributed binning," *info*, vol. 51, pp. 3457 – 3474, October 2005.

[46] S. M. Kay, *Modern Spectral Estimation: Theory and Applications*. Englewood Cliffs, NJ: Prentice-Hall, 1988.

[47] J. D. Markel and A. H. Gray, *Linear prediction of speech*. New York: Springer-Verlag, 1976.

[48] A. V. Oppenheim and R. W. Schafer, *Discrete-time signal processing*. Prentice Hall, 1989.